RECEIVED BY TIC MAR 8 1978

NUREG/CR-0018
UVA/529058/NEEP77/103

POST-FAILURE PHENOMENA IN LMFBR TOP ACCIDENTS

MASTER

Final Report
October 1, 1976 - September 30, 1977

C. A. Erdman D. R. Bradley
J. L. Kelley

University of Virginia

Prepared for
U. S. Nuclear Regulatory Commission

DISTRIBUTION OF THIS DOCUMENT IS UNLIMITED

DISCLAIMER

This report was prepared as an account of work sponsored by an agency of the United States Government. Neither the United States Government nor any agency thereof, nor any of their employees, makes any warranty, express or implied, or assumes any legal liability or responsibility for the accuracy, completeness, or usefulness of any information, apparatus, product, or process disclosed, or represents that its use would not infringe privately owned rights. Reference herein to any specific commercial product, process, or service by trade name, trademark, manufacturer, or otherwise does not necessarily constitute or imply its endorsement, recommendation, or favoring by the United States Government or any agency thereof. The views and opinions of authors expressed herein do not necessarily state or reflect those of the United States Government or any agency thereof.

DISCLAIMER

Portions of this document may be illegible in electronic image products. Images are produced from the best available original document.

NOTICE

This report was prepared as an account of work sponsored by the United States Government. Neither the United States nor the United States Nuclear Regulatory Commission, nor any of their employees, nor any of their contractors, subcontractors, or their employees, makes any warranty, express or implied, nor assumes any legal liability or responsibility for the accuracy, completeness or usefulness of any information, apparatus, product or process disclosed, nor represents that its use would not infringe privately owned rights.

Available from
National Technical Information Service
Springfield, Virginia 22161
Price: Printed Copy$6.00 ; Microfiche $3.00

The price of this document for requesters outside of the North American Continent can be obtained from the National Technical Information Service.

NUREG/CR-0018
UVA/529058/NEEP77/103

POST-FAILURE PHENOMENA IN LMFBR TOP ACCIDENTS

Final Report
October 1, 1976 - September 30, 1977

C. A. Erdman D. R. Bradley
J. L. Kelley

Manuscript Completed: November 1977
Date Published: February 1978

University of Virginia
School of Engineering and Applied Science
Charlottesville, VA 22901

Prepared for
Division of Project Management
Office of Nuclear Reactor Regulation
U. S. Nuclear Regulatory Commission
Under Contract No. AT(49-24)-0158

DISTRIBUTION OF THIS DOCUMENT IS UNLIMITED

TABLE OF CONTENTS

TABLE OF CONTENTS CONT'D.

ABSTRACT

Contract work of FY77 for NRC's Division of Project Management in the area of post-failure phenomena in LMFBR TOP accidents is reported. Several different TOP-related topics are treated.

Topics include radial dependence of transient fission gas behavior in LMFBR pins; modeling of flowing-sodium pin failure tests in TREAT; gas plenum region pressurization due to sodium vaporization; and the effect of ejection rates of molten fuel from failed pins on the potential for extensive subassembly voiding.

A review of other FY77 work, including previous topical reports, is provided in addition to a summary and recommendations section.

1. SUMMARY AND RECOMMENDATIONS

This final report marks the termination of a continuous period of almost six years during which the Nuclear Engineering and Engineering Physics Department (formerly Nuclear Engineering Department) of the University of Virginia has performed contractual services for the LMFBR Branch of the Division of Project Management of the NRC and the corresponding branch of the AEC (predecessor to NRC). A chronological listing of some of the reports required by these contracts is given as Reference 1 at the end of this introductory section.

During the fiscal year just past, emphasis was placed on a continuation of work initiated in FY76. That work was primarily aimed at establishing minimum requirements for extended subassembly voiding. The interest in extended voiding has been tied to the role of such voiding in contributing to development of blockages in the unprotected transient overpower (TOP) accident. The expansion of our FY77 work to areas other than those of FY76 is reflected in the variety of topics considered in this report. However, all topics clearly fall under the scope of the contract title: "Post-Failure Phenomena in LMFBR TOP Accidents."

Calculations of radially dependent transient gas release were made using Gruber's PFRAS[2] model. LOF and LOF-Driven-TOP channels from a SAS3A run for CRBR were examined. It is clear from the results of those calculations (presented in Section 2.6 of this report) that a single-radial-node representation of unrestructured fuel in transient gas release calculations can be misleading. A multinodal approach can predict overall larger transient releases to a given time in the transient and will also predict a severe redistribution of remaining gas toward the outer rind of unrestructured fuel. For LOF channels this means that less total gas is present in the fuel at initiation of slumping and that the remaining gas may not be easily available to contribute to dispersal. For the TOP channels, the multi-radial-node

analysis predicts larger released gas inventories at pin failure. The recommendation is made that radial dependence of gas release be considered in future transient analyses.

TREAT 7-pin test geometry and associated hydraulics were examined as a followup to previously reported work[1.c] on the single pin TREAT test H2. The TREAT test calculations have provided increased confidence in analysis tools used in full subassembly analyses. The mildness of H2 results appears, as suggested by Cronenberg,[3] to be the result of substantial prefailure boiling or very small initial fuel releases which created a significant void fraction in the region around the failure site into which later fuel ejection occurred. Thus substantial liquid-liquid contact between fuel and sodium never occurred; such an occurrence might be less likely with irradiated pins in the TREAT MARK-IIA loop environment or with either fresh or irradiated pins in more prototypic subassembly conditions. In looking at H5 it was found that, indeed, a one-of-seven failure would be expected to produce mild results as observed experimentally. The MARK IIA test loop was found, when compared with subassembly conditions under the same strength FCI, to show greater ease of voiding initiation but a relative immobility of the interaction zone. These factors suggest a greater facility for development of blockages in the MARK-IIA loop relative to subassembly conditions. Analyses of multiple pin tests under full flow, full head conditions are recommended.

The ANL Upper Plenum Injection (UPI) tests were reviewed. Simple verifying calculations were performed when possible. The primary document utilized was the paper presented at Chicago in October 1976. Some ANL monthly progress reports and other limited distribution reports were also examined. The major conclusion reached in this review was that it seems unlikely that sodium vaporization was a primary pressurization source in the tests. However, the likelihood of such an occurrence was essentially precluded by the nature of the thermite mixture and its injection process. Void fractions at impact of the thermite mixture and sodium were extremely large in UPI #1.

Moreover, the void did not consist of fuel vapor but rather non-condensable gas. Close examination of planned and/or completed simulant tests is recommended; however, a better experiment using reactor materials is also needed.

A brief review of work previously reported in topical reports[1.c,1.d] was also performed in preparation of this final report. Special attention was given to voiding in the LOF-Driven-TOP without compensating fuel motion feedback. It was emphasized that various degrees of fuel/sodium energy and momentum coupling and of communication between pin cavity and coolant channel could produce such voiding. Recommendation is made for further work in this area. Other conclusions from the topicals were that plenum gas voiding of sodium is not likely to be of interest in the classical TOP accident and that, although sodium voiding can be extensive in the LOF-Driven-TOP, the time scales for voiding would not allow it to be a major source for reactivity insertion. The indirect effect of gas driven voiding in the LOF-Driven-TOP on the overall sequence of events may be important, however, and should be examined.

The importance of fuel ejection rates on resulting void development was also examined in FY1977. The motivation for this work (i.e. possible obstructions behind the failure) is discussed in Reference 1.d. Ejection rates from failed pins were arbitrarily reduced by factors of five and more relative to values predicted by pin mechanics models (e.g. Reference 5). Such reductions were still not sufficient to eliminate significant voiding under subassembly conditions; however, another factor-of-two reduction would seem to be sufficient and should be examined to complete the scoping calculations on the effect of fuel ejection rates.

Efforts at modeling of possible plenum pressurization due to sodium vaporization met with little success in FY77. It was quickly determined that the level of sophistication needed in such a model to even begin to approximate the physical processes was well beyond the charge of the contract effort. Some

simple upper-limit calculations were performed to examine the range of fuel-void-fractions where pressurization might be precluded. Recommendations were made to attempt to utilize existing codes (e.g. SIMMER-I[6]) in which the key exchange coefficients can be selected consistent with the physical situation under consideration. There would seem to be no point in separately assembling another parametric model.

SECTION 1 REFERENCES

1a. A. B. Reynolds and C. A. Erdman, "Fuel Coolant Interaction in LMFBR Accident Analysis," Research Laboratories for the Engineering Sciences Reports, University of Virginia, Charlottesville, Virginia

First Quarterly Report, ORO-4313-1 (March 1972).

Second Quarterly Report, ORO-4313-2 (June 1972).

Third Quarterly Report, ORO-4313-3 (October 1972).

Fourth Quarterly Report, ORO-4313-4 (February 1973).

Fifth Quarterly Report, ORO-4313-5 (May 1973).

Sixth Quarterly Report, ORO-4313-6 (August 1973).

Seventh Quarterly Report, ORO-4313-7 (November 1973).

Eighth Quarterly Report, ORO-4313-8 (February 1974).

Nineth and Tenth Quarterly Reports, ORO-4313-9,10 (September 1974).

Eleventh and Twelfth Quarterly Reports, ORO-4313-11,12 (June 1975).

Thirteenth and Fourteenth Quarterly Reports, ORO-4313-13,14 (July 1975).

1b. C. A. Erdman, M. B. Johnson, and A. B. Reynolds, "Post-Failure Phenomena in LMFBR TOP Accidents," Department of Nuclear Engineering, Research Laboratories for the Engineering Sciences, University of Virginia, Charlottesville, Virginia.

Quarterly Progress Report, July 1, 1975 - September 30, 1975.

Quarterly Progress Report, October 1, 1975 - December 31, 1975.

Quarterly Progress Report, January 1, 1976 - March 31, 1976.

Annual Report, July 1, 1975 - June 30, 1976.

1c. C. A. Erdman and M. B. Johnson, "Some Aspects of Subassembly Voiding in the Unprotected Transient Overpower Accident in LMFBR's," NUREG-0277 (June 1977).

1d. C. A. Erdman and M. B. Johnson, "Some Aspects of Fuel Motion in the Unprotected Transient Overpower Accident in LMFBR's," NUREG-0282 (June 1977).

2. E. E. Gruber, "A Generalized Parametric Model for Transient Gas Release and Swelling in Oxide Fuels," Submitted for Publication to the Journal of Nuclear Technology (1977).

3. A. W. Cronenberg, "A Thermodynamic Model for Molten UO_2-Na Interaction Pertaining to Fast-Reactor Fuel-Failure Accidents," ANL-7947 (June 1972).

4. R. E. Henry et al., "Experiments of Pressure-Driven Fuel Compaction with Reactor Materials," Int. Mtg. on Fast Reactor Safety and Related Fields, CONF-761001, Vol. IV, pp. 1734-1743 (October 1976).

5. P. A. Pizzica and P. B. Abramson, "EPIC: A Computer Program for Fuel-Coolant Interactions," loc. cit. 4, Vol. III, pp. 979-987.

6. L. L. Smith et al., "SIMMER-I, an LMFBR Disrupted Core Analysis Code," loc. cit. 4, pp. 1195-1202.

2. RADIALLY DEPENDENT GAS RELEASE CALCULATIONS

2.1 Introduction

In order to accurately model the response of irradiated fuel pins to a thermal transient, fission gas behavior must be considered. Gas which is released to grain boundaries can contribute to fuel breakup or motion, and gas retained within the grains can cause significant intragranular swelling. The FRAS family of codes is being developed by E. E. Gruber[1,2,3,4] to model this transient gas release and swelling. Here at U.Va. we have utilized a parametric version of FRAS described in Reference 4 to look at the details of transient behavior of fuel gases during the loss-of-flow (LOF) accident and the loss-of-flow-driven-transient-overpower (LOF-Driven-TOP) accident in CRBR.

Fission gas is important as a potential dispersal mechanism in the highest power subassemblies which undergo disruption first in the LOF accident. In the LOF-Driven-TOP, fission gas is the major driving force for ejection of fuel from failed pins and also offers the potential for direct sodium voiding. Analyses[5] of these accidents have partially accounted for the influence of transient-released fission gas; however, the unrestructured fuel which contains most of the gas at steady state has usually been treated as a single radial zone at a given axial node in calculating gas releases. One temperature and one gradient have been used in calculating releases at a given axial location. We have felt that this simplification gives a misleading picture of the gas available at initiation of fuel slumping in the LOF and at pin failure in the LOF-Driven-TOP.

In the LOF, the gas retained at slumping initiation will predominantly be in a very thin, relatively cold outer "rind" of the fuel pellets. Gas originally in the inner regions of the unrestructured fuel will have been released prior to slumping because of the significantly higher temperatures of the inner region during the transient.

The remaining unreleased gas, which is principally in the outer rind of fuel, may be sufficiently separated from the molten fuel to prevent its acting as a strong dispersal mechanism on time scales of interest. In the TOP subassemblies of the LOF-Driven-TOP, a similar sort of non-uniform release of gas from the unrestructured fuel will occur. Here we were more concerned with the total amount of gas that would be released up to the time of pin failure.

In order to perform the analyses described above, it was necessary to create a simple computer code based on the PFRAS (parametric FRAS) description given in Reference 4. This report contains a brief description of FRAS and PFRAS, a discussion of the verification of the code used at U.Va., and the results of the radially dependent gas release calculations.

2.2 Mechanistic Approach to Fission Gas Release and Swelling - FRAS

The following is an overview of Gruber's models of transient fission gas behavior[1,4]. The underlying assumption in Gruber's work is that, during steady state operation, a network of interlinked porosity will develop such that fission gas release is controlled by the rate at which gas reaches the grain boundaries. Therefore, only intragranular motion is examined. Other investigators[6] have recently looked at the rate processes involved in the subsequent gas behavior, but we will not consider those processes here.

Several other important assumptions should also be mentioned here. Fission gas is assumed to be retained initially as a super-saturated solid solution of individual gas atoms within spherical grains. Composition and material properties are assumed to be constant across the pin. The effects of dislocations within grains are ignored, even though they may be significant in the early stages of the transient. During the transient, fission gas precipitates rapidly into stable bubbles which move within the grains. These bubbles can do two things. They can coalesce with one another, and they can migrate to grain boundaries, where they are trapped. This migration is assumed to take place by surface diffusion, a process in which the motion of atoms along the inner surface of the bubble produces a net motion of the center of the bubble. These atoms are originally attached to the surface but may acquire enough energy to mobilize and move along the surface before becoming bound again.

In the presence of a thermal gradient, the motion of the surface atoms will be in the direction of lowest temperature; thus the net motion of the bubble will be in the direction of highest temperature. In a fuel pin, for example, the motion of fission gas within grains would be towards the center. In addition to this "biased" migration, a degree of random migration takes place which is independent of the temperature field.

As noted before, during migration the bubbles are also coalescing with one another. Gruber's model simplifies the coalescence phenomenon by assuming that the equilibrium bubble size is achieved instantaneously after contact. The validity of this argument will be discussed later in this report. As coalescence takes place, the bubble size distribution will shift with time toward larger bubbles, resulting in a significant degree of swelling. Gruber's fission gas release and swelling code, FRAS, calculates the evolution of the bubble size distribution by a "binning" procedure. In FRAS, bubbles are grouped into "bins" of discrete size intervals. As two bubbles coalesce, a product bubble is formed which is "placed" into a bin of larger size.

Each bubble size has associated with it a specified migration velocity. For a given time step, FRAS averages the bubble velocities over the entire size distribution to get a mean bubble velocity. Since one would expect migration to the grain boundaries to depend on bubble mobility, i.e. velocity, there should be some way to relate the amount of gas released to the mean velocity.

Gruber's concept of gas release is best illustrated by the simple geometric model shown in Figure 2.1[1]. The dashed-line sphere represents a conceptual envelope for the migrating fission gas. The solid-line sphere is the spherical grain of radius a. The overlap between the spheres represents the volume of unreleased gas. The cumulative migration distance, ℓ, is calculated by integrating the mean velocity over the transient time. The overlap distance is represented by h.

Using a simple geometric analysis, Gruber arrived at the gas release fraction by biased migration,

$$f_b = 1 - \frac{h^2\ (3a - h/2)}{8a^3}$$

For gas release via random migration, Gruber used the analysis

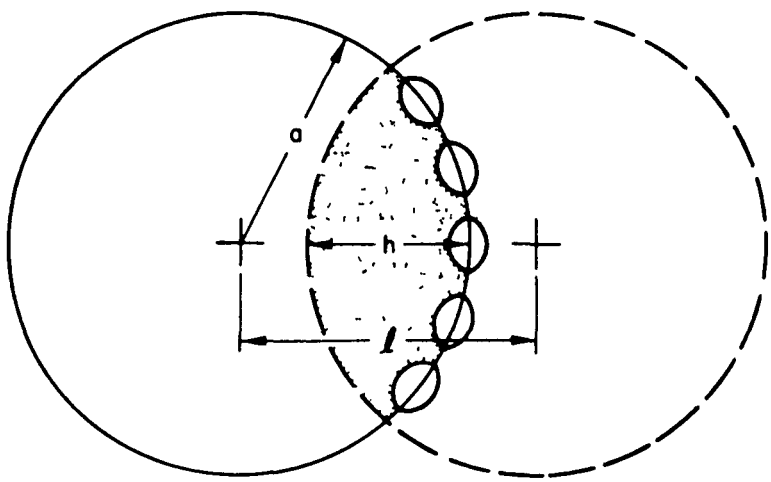

Figure 2.1 Schematic Illustration of Gruber's Biased Release Model (Reproduced from Ref. 1).

of J. Crank[7] for diffusion of solute from a sphere, with the approximation proposed by J. M. Kennedy, as referenced by A. H. Booth[8],

$$f_r = \cong 6\ (Dt/\pi a^2)^{1/2} - 3\ Dt/a^2 \quad ,$$

where D is the bubble diffusivity, and t is the transient time.

The change in volume due to intragranular swelling is found by summing the bubble volumes, assuming no gas release, and then correcting for release by multiplying by $(1 - f_b - f_r)$. The swelling analysis that Gruber uses is only accurate when the predicted swelling is small (< 30%)[4]. This is a result of the inaccuracy of several simplifying assumptions that were made in the formulation of the model such as: a) bubbles are assumed to be isolated; b) coalescence takes place immediately upon contact between two bubbles; c) time for product bubbles to reach equilibrium size is ignored; and d) the effects of pinning by dislocation and resolution are neglected. Large values of predicted swelling indicate a likelihood that gross swelling would occur, but should not be interpreted quantitatively.

2.3 Parametric Approach to Fission Gas Release - PFRAS

Because the FRAS code is prohibitively expensive for the type of multinodal analyses required in fuel behavior and safety studies, it was necessary to simplify the calculations greatly. In his parametric FRAS code, PFRAS[4], Gruber has successfully synthesized FRAS results by a simplified analytical method which utilizes a few easily calculable parameters. The discussion given below is derived primarily from Reference 4.

Preliminary calculations with FRAS showed that biased migration is by far the dominant process; therefore, Gruber directed his attention toward an explicit treatment of biased migration release, with random migration included implicitly.

Fundamental to this analysis is the dimensionless time, τ, which is derived from the biased migration analysis;

$$\tau = \left(\frac{3\,\pi}{2\,\gamma\,k} \right)^{1/2} \Omega\,\nu\,Q_s\,C_o \int_o^t \frac{D_s\,\Delta T_s\,dt'}{T^{3/2}\,(1 + \Delta V)}$$

where Ω is the molecular volume and Q_s is the surface diffusion heat of transport. The importance of τ will be evident shortly.

Gruber found that the mean migration velocity could be given by:

$$\bar{V} = \frac{\mu\,D_s\,\Delta T_s}{T^{5/2}\,\tau} \quad ^*,$$

---

*D_s is given by: $D_s = 3.5 \times 10^4 \exp(-90/RT)$ where RT has dimensions (kcal/mole); ΔT_s is the temperature gradient at the bubble surface. For a non-heat-conducting bubble, this can be approximated by 3/2 ΔT, where ΔT is the bulk thermal gradient[4].

where μ is a parameter that is a function of pressure, P, and dimensionless time only. Using FRAS results for a variety of conditions, μ was specified in a two-dimensional table[4] in terms of P and τ.

Similarly the fractional swelling (without the gas release correction) could be given by:

$$\Delta V = \phi \, T^{3/2} \, C_o \, \tau \quad ,$$

where ϕ is another parameter which is a function of P and τ only. Again FRAS results were used to provide a two-dimensional table[4] for ϕ.

Using $\bar{V}$, fractional release via biased migration could be determined and intragranular swelling calculated by:

$$\Delta V' = (1 - f_b) \, \Delta V \quad .$$

Biased migration is treated explicitly in this analysis, and since μ and ϕ are based on FRAS results which include both f_b and f_r, random migration is treated implicitly.

2.4 Attempt to Duplicate PFRAS Code Results - FISGAS

In order to perform calculations using the PFRAS model, a small code named FISGAS was written at U.Va. FISGAS relies mainly on a combination of the subroutine DIFFSYS[9], a differential equation solver using the Bulirsch-Stoer method[10], and DIFFDRV[11], a general main program used to drive DIFFSYS. Only slight modification of DIFFDRV was necessary to create the main program, FISGAS. FISGAS accepts input, calls DIFFSYS, calculates gas release and swelling, and controls output. In order to use DIFFSYS, a subroutine, DIFFUN, must be written by the user to specify the differential equations to be solved. Also, the function subprogram, ENTRP, is used by FISGAS to do a two-dimensional logarithmic interpolation for μ and ϕ as part of the calculation for gas release and swelling.

In order to test the operability of the FISGAS code, an attempt was made to duplicate several of the cases that were run by Gruber in testing PFRAS[4]. FISGAS results could then be compared with FRAS and PFRAS results. The results of test cases used in our comparison provide a demonstration of the ability of the PFRAS/FISGAS codes to reproduce FRAS results and of the sensitivity of transient fission gas behavior to the parameters considered. The base case parameter values used were these: 300° C/s heating rate (varied from 100 to 1000); 5000° C/cm thermal gradient (varied from 1000 to 25000); 10 micron grain diameter (varied from 4 to 25); 1 x 10^{20} gas atoms/cc initial fission gas concentration (varied from 0.2 to 4 x 10^{20}); and 0.25 MPa pressure (varied to 8.61 and 141.86). FISGAS results showed excellent agreement with Reference 4 results. One comparison is shown in Figure 2.2. This was perhaps the worst agreement noted in any of the comparisons and may be due more to plotting problems than to calculational results.

2.4.1 Generalization of FISGAS to Allow for Time-Dependent Input

After determining that the solution method in FISGAS was correct, the next step was to generalize the code so that any transient of interest could be modeled. In order to accomplish this, the input format had to be modified to allow for time-dependent variation of temperature, pressure, and temperature gradient.

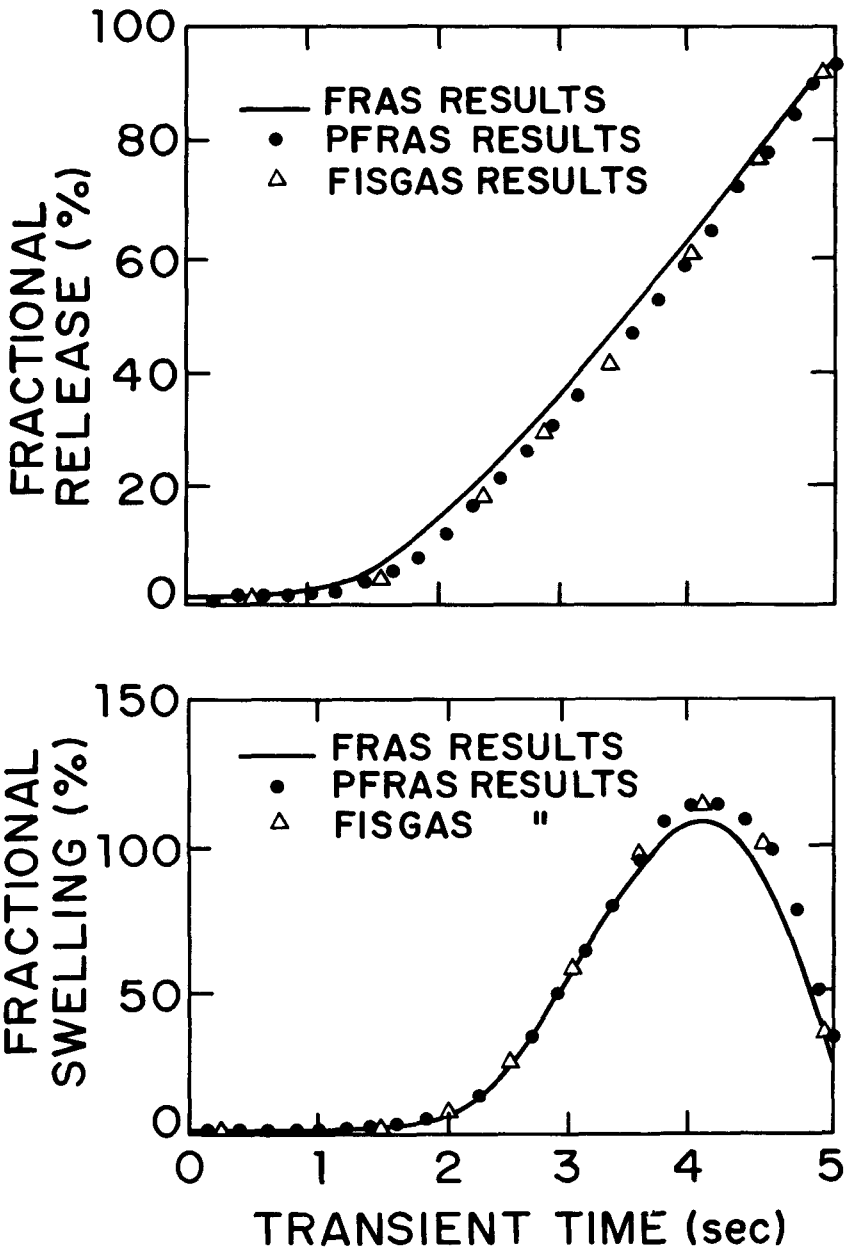

Figure 2.2 Comparison of FISGAS Results with FRAS and PFRAS Results for Case With Extreme Thermal Gradient (2500°C/mm).

In determining how this modification might best be achieved, three things had to be considered. First, raw data from the transient should be easily convertible to a form suitable for input to the code in order to minimize user effort. Secondly, computer time should be minimized in order to minimize cost. Finally, accuracy in modeling the transient should be maximized.

The transient data of interest to us were taken from a SAS3A simulation of a LOF accident in CRBR. The SAS3A results were similar to results presented by NRC staff in Reference 5. The information needed from this SAS run included temperatures at various axial and radial fuel nodes, radial fuel mesh structure at each axial location, and pin cavity pressure. In order to determine the temperature gradient at a given node, central differencing was used for all interior nodes, and backward differencing, for the outer node. The nodal arrangement is shown in Figure 2.3.

For the initial transient study, channel 7 was chosen, because it was the first channel to undergo a transient-over-power accident as a result of the loss-of-flow in higher power channels. Axial nodes 11 and 14 were chosen for individual study because they represent the highest power node and uppermost central void node respectively. Since empirical results have shown that most of the fission gas in a fuel pin is concentrated in the unrestructured fuel region, only the nodal locations which represent unrestructured fuel were examined. For axial node 11, this region consisted of radial nodes 9 and 10; for axial node 14, this region consisted of radial nodes 8, 9, and 10; for the remainder of this report, the various fuel nodes and corresponding computer runs will be referred to as follows: 7-11, 9; 7-11, 10; 7-14, 8; and 7-14, 10. Similar nomenclature will be used for other nodes and calculations.

At specified times during the transient, SAS3A prints out the transient temperature for each axial-radial location. Also given is

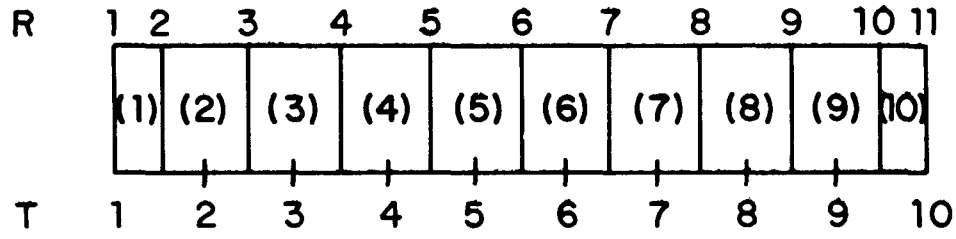

R= RADIAL MESH POINTS

T= RADIAL TEMPERATURE MESH POINTS

( ) DENOTES RADIAL NODE NUMBERS

NOTE THAT NODES (1) AND (10) ARE HALF- SIZE NODES

Figure 2.3 Fuel Pin Nodal Structure for SAS3A Heat Transfer Calculations.

the radial fuel mesh at each axial location. From this the temperature gradients are calculated as follows:

$$\nabla T_8 = \frac{T_9 - T_7}{\frac{R_9 + R_{10}}{2} - \frac{R_7 + R_8}{2}} \quad ;$$

$$\nabla T_9 = \frac{T_{10} - T_8}{R_{11} - \frac{R_8 + R_9}{2}} \quad ;$$

$$\nabla T_{10} = \frac{T_{10} - T_9}{R_{11} - \frac{R_9 + R_{10}}{2}}$$

The internal pin pressures for each pin (channel) are also calculated by SAS. These pressures are assumed the same for each axial-radial location in the pin.

Once the transient temperature, pressure, and temperature gradient data were collected, the next step was to decide how to transform this information into a form suitable for input to FISGAS.

Various approaches for processing the transient data were tried. Several attempts were made at curve fitting and ultimately rejected in favor of a tabular form for treating the data. The version of FISGAS utilizing the table approach was designated FISGAS3. Between the times for which input is specified, the code interpolates linearly for T, P and ∇T by adding the incremental value, $\frac{dY^*}{dt} \cdot \nabla T$, to the previous value. Here $\frac{dY}{dt}$ (the value used by DIFFSYS) is calculated for each time interval, t_i to t_{i+1}, as $\frac{Y_{i+1} - Y_i}{t_{i+1} - t_i}$, and Δt is the time

---

*Y is a general representation for T, P, and ∇T.

step used by DIFFSYS. Computational difficulties were anticipated because of the discrete changes in the derivatives of P, T and ∇T inherent in use of a table.

As a quick check of the method used in FISGAS3, an attempt was made to match a set of test case results shown in Figure 16 of Reference 4. This case was a variation of the base case (see page) with the following simple time dependent pressure variation: between 1 and 4 seconds the pressure is increased linearly from 0.25 MPa to 121.6 MPa, simulating gap closure and cladding pressurization of the fuel; from 4 to 5 seconds the pressure is decreased linearly back to 0.25 MPa simulating cladding failure and stress relaxation in the fuel.

The results of this FISGAS3 run are shown in Figure 2.4. The gas release and swelling curves appear to be identical to the FRAS/PFRAS results, at least to the accuracy with which the curves from Reference 4 can be read. It appears, therefore, that FISGAS3 is an accurate duplication of Gruber's PFRAS code.

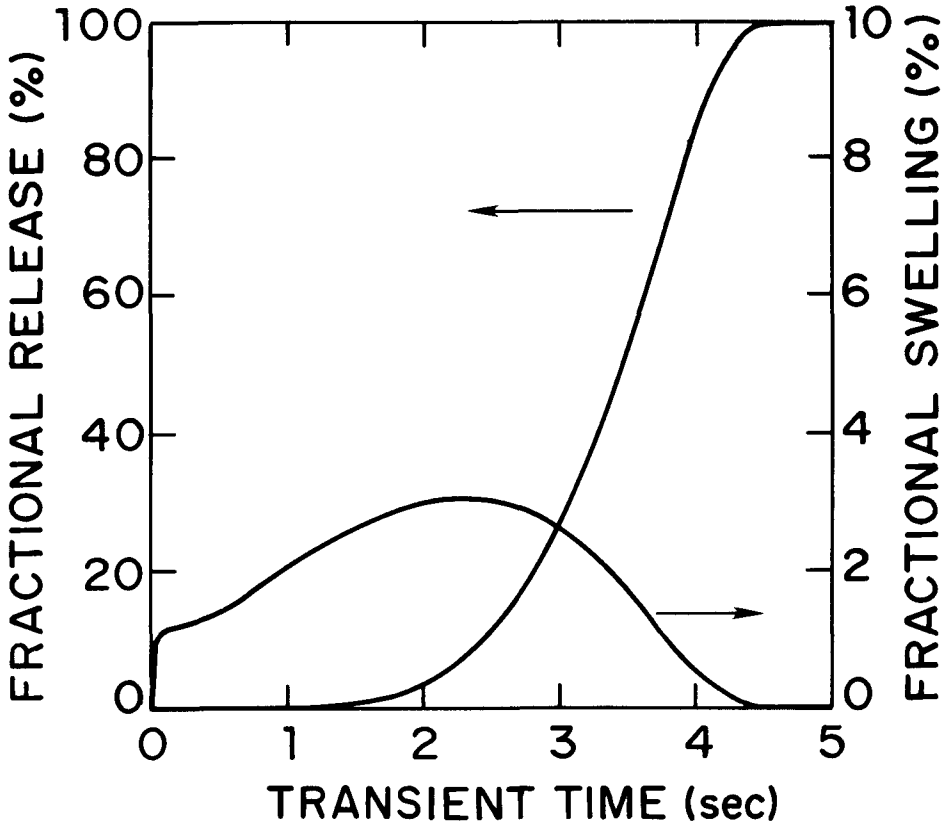

Figure 2.4 FISTAS Results for Case from Reference 4 which Considers Time-Dependent Pressure Variation. Results Appear Identical to those of Reference 4.

2.5 Comparison of FISGAS3 and SAS Results

The SAS3A run used to obtain transient data also provided results of single radial zone gas release calculations using an earlier, less general parametric model[2,3] based on FRAS. We felt it would be useful to perform a comparison calculation using FISGAS3 to check on the validity of the simpler parametric model in SAS.

Since the SAS calculation is based on average values of T,P, and ∇T for the unrestructured region, these averages had to be computed before the equivalent FISGAS3 run could be made. In addition, it should be noted that the parametric relationships used in SAS to predict release and swelling are based on a 4 micron grain diameter, and not the typically accepted values of 10 microns.

The cases which were run in order to compare FISGAS3 and SAS results, were designated 7-11, U(4) and 7-14, U(4). U refers to the averaging of quantities over the unrestructured region and (4) flags the smaller grain size. The gas release vs. time results for channel 7 shown in Figure 2.5 illustrate the excellent agreement between SAS and FISGAS3 results for this transient.

This comparison was continued by next looking at fission gas release and swelling for channel 2. Channel 2 was chosen because it was the first channel to slump during the loss-of-flow transient. In choosing which nodes to study, the same criteria were used for channel 2 as for channel 7. Again the highest power axial node was 11, with unrestructured radial nodes 9 and 10. Also, the highest central void node was again 14 with unrestructured radial nodes 8, 9 and 10.

The process of preparing data for use in the SAS-FISGAS3 comparison cases (2-11, U(4) and 2-14, U(4)) also created input for four other cases: 2-11, 9; 2-11, 10; 2-14, 8; and 2-14, 10. The results of these four cases will be discussed later in conjunction with the results of the corresponding channel 7 cases.

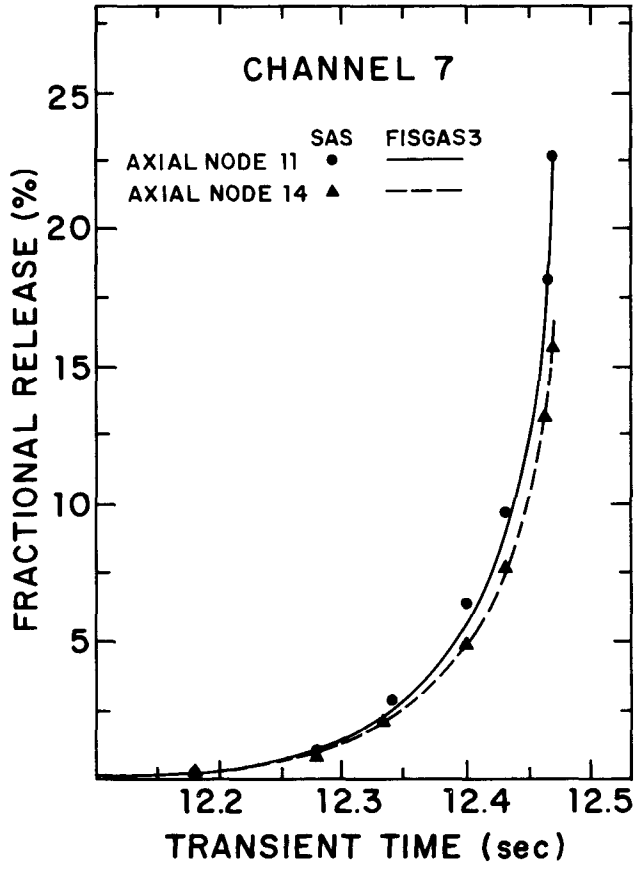

Figure 2.5 Comparison of SAS and Single-Radial-Node FISGAS Results [7-11, U(4) and 7-14, U(4)] for Channel 7

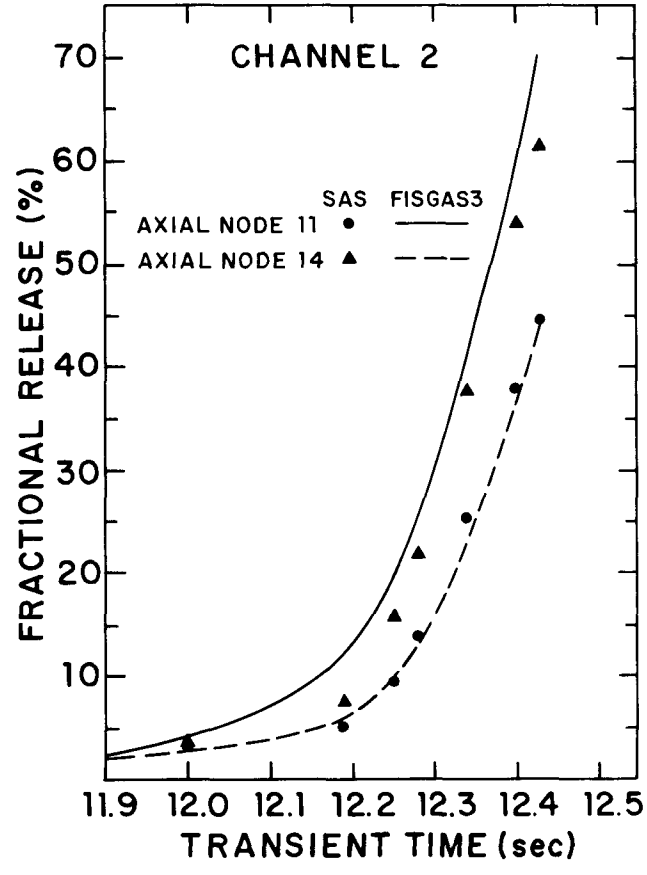

Figure 2.6 Comparison of SAS and Single-Radial-Node FISGAS Results [2-11, U(4) and 2-14, U(4)] for Channel 2.

The comparisons of SAS and FISGAS3 results for channel 2 are shown in Figure 2.6. As with both channel 7 cases, case 2-14, U(4) is in good agreement with the SAS calculation. Gas release from case 2-11, U(4), however, varies from the corresponding SAS calculation by a significant amount ($\sim$ 12.4%). At this time, all that can be said in explanation of this fact is that the parametric equation upon which the SAS calculation is based is only an approximation, and that the accuracy of this approximation depends greatly on the transient being modeled. Though no specific accuracy limitations have been identified, early development of this parametric method showed that its accuracy drops off somewhat for low ($\lesssim$ 10%) and high ($\gtrsim$ 50%) values of gas release[3].

2.6 Calculation of Radial Dependence of Gas Behavior

The discussions in the previous sections have mainly been preliminary in nature, designed to provide background needed for the discussions of this section. The primary objective in our work with PFRAS and FISGAS3, as indicated in the introduction to this report, was to investigate the radial dependence of transient gas release and swelling within the initially unrestructured fuel at a given axial location. This dependence is clearly illustrated in Figures 2.7 through 2.14. Each figure applies to a single axial mode of one channel. The transient conditions utilized (i.e., temperature and pressure histories) were taken from the SAS3A run mentioned in Section 2.5 which modelled the LOF accident in CRBR.

Release and swelling results are shown at each axial mode examined for the innermost and outermost radial modes of the unrestructured region. Also shown in each figure are the results of a SAS-like thermal averaging of all radial modes of unrestructured fuel (labelled "single node calculation"). Note that a true mass-averaged value for release or swelling can be obtained from axial node 11 results by performing a mass-weighted average of the results of runs 7-11, 9 and 7-11, 10 or from 2-11, 9 and 2-11, 10. This type of mass-weighted results (labelled "weighted average") is shown in Figures 2.7, 2.8, 2.11, and 2.12. We will first discuss the channel 7 results presented in Figures 2.7 through 2.10. The calculations involved here and for the remainder of the report all assumed a 10 μm grain size.

Channel 7 was the first TOP channel to fail. Failure might well extend from above axial node 14 all the way down well past the core midplane. This means that axial nodes 11 and 14 (among others) must be properly characterized. From Figure 2.7 we see that, as expected, the fractional gas release from radial node 9 at axial node 11 (referred to as 7-11, 9) is an order of magnitude greater than for

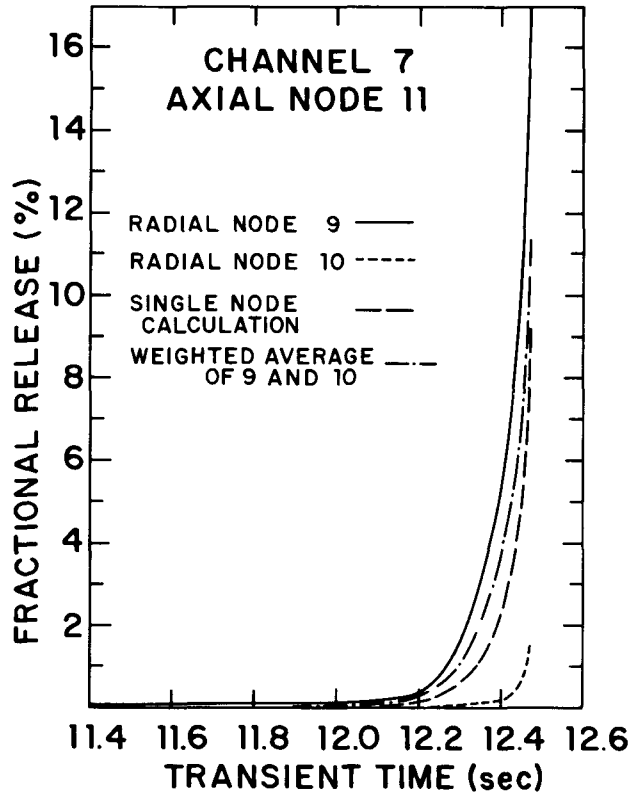

Figure 2.7 Predicted Releases for Axial Node 11 of Channel 7, Illustrating Radial Dependence and Error Involved in Single Radial-Node Calculation.

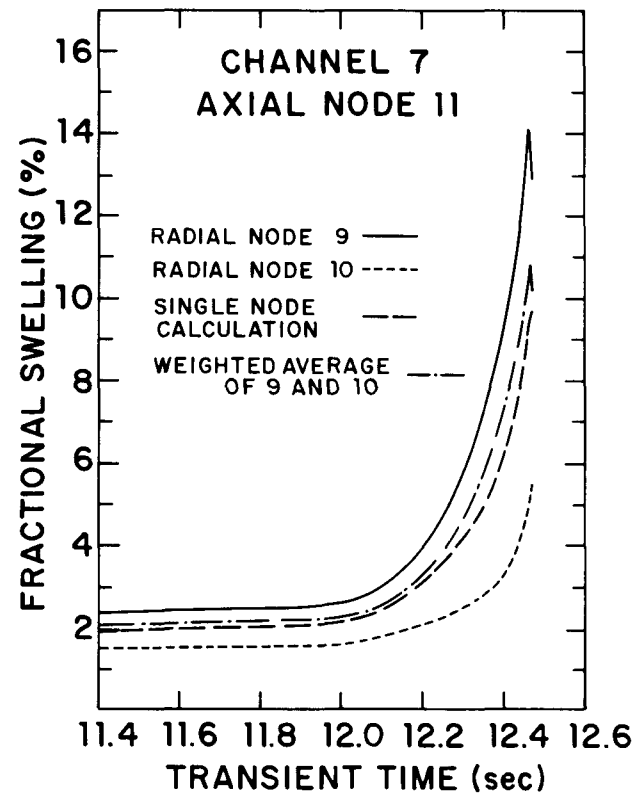

Figure 2.8 Predicted Swelling for Axial Node 11 of Channel 7, Illustrating Radial Dependence and Error Involved in Single Radial-Node Calculation.

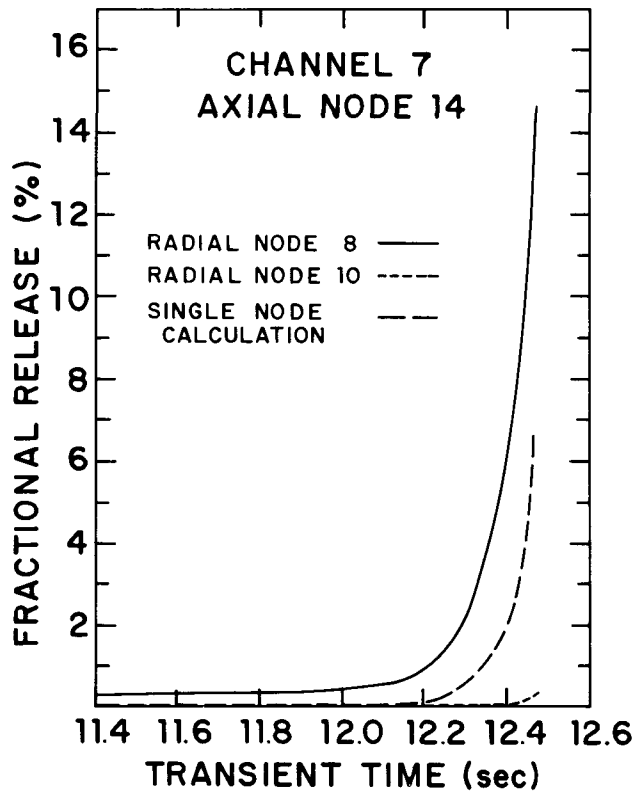

Figure 2.9 Predicted Releases for Innermost and Outermost Unrestructured Radial Nodes in Axial Node 14 of Channel 7. Single-Radial-Node Results are Given for Comparison.

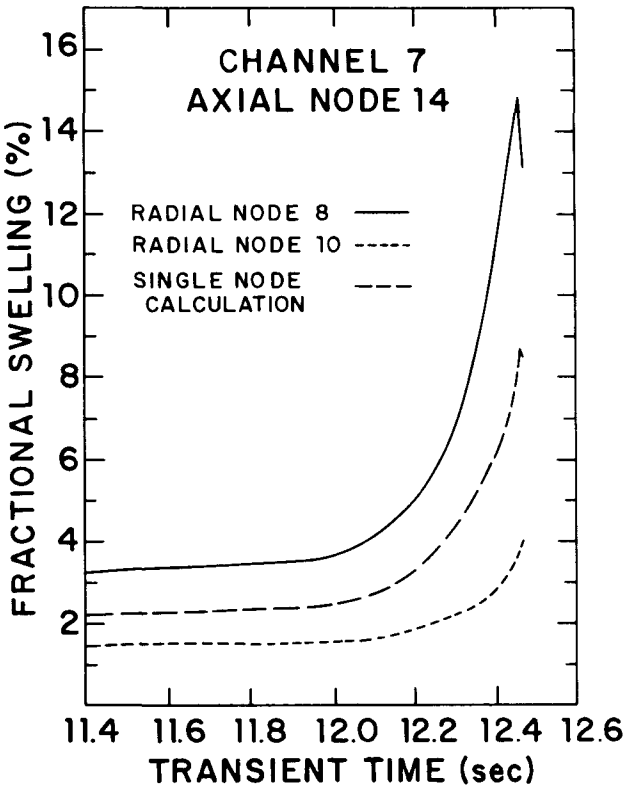

Figure 2.10 Predicted Swelling for Innermost and Outermost Unrestructured Nodes in Axial Node 14 of Channel 7. Single-Radial Node Results are Given for Comparison.

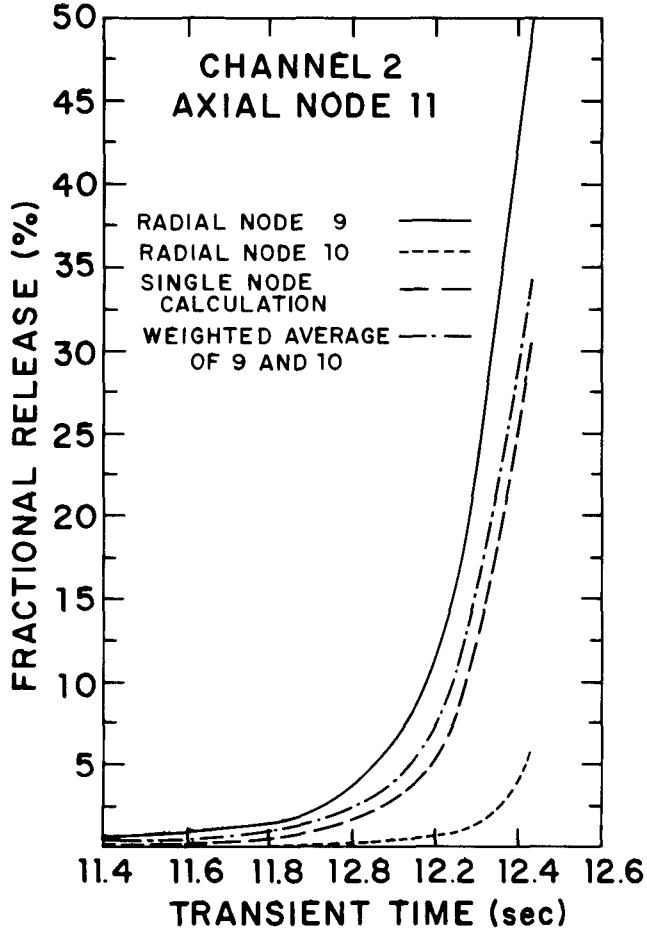

Figure 2.11 Predicted Releases for Axial Node 11 of Channel 2, Illustrating Radial Dependence and Error Involved in Single-Radial-Node Calculation.

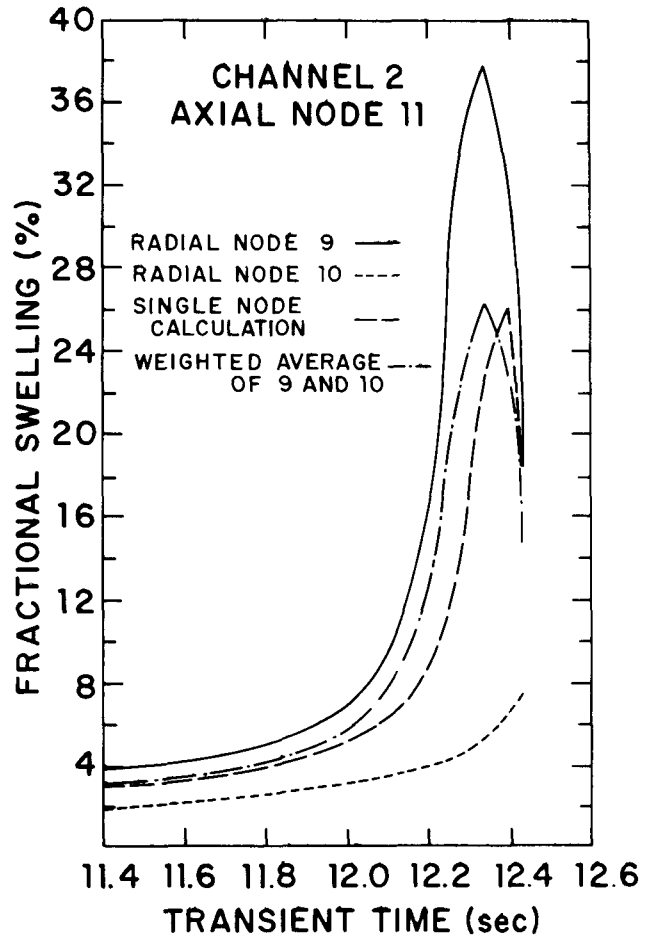

Figure 2.12 Predicted Swelling for Axial Node 11 of Channel 2, Illustrating Radial Dependence and Error Involved in Single-Radial-Node Calculation.

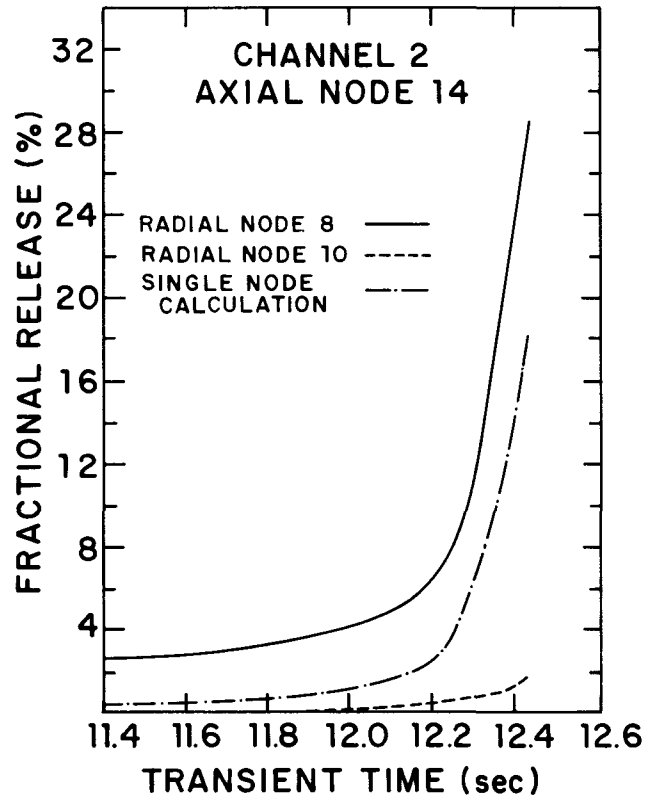

Figure 2.13 Predicted Releases for Innermost and Outermost Unrestructured Radial Nodes in Axial Node 14 of Channel 2. Single-Radial-Node Results are Given for Comparison.

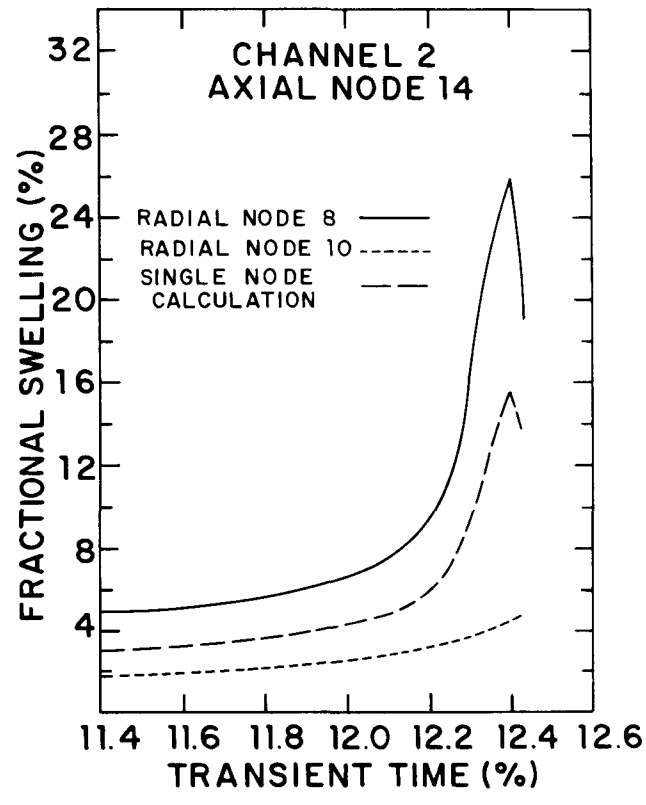

Figure 2.14 Predicted Swelling for Innermost and Outermost Unrestructured Radial Nodes in Axial Node 14 of Channel 2. Single-Radial-Node Results are Given for Comparison.

node 7-11, 10. At termination of the SAS calculation, releases for those nodes were 16.7% and 1.49%. This should be compared to a predicted release of 9.16% when the unrestructured region is treated as a single radial zone (case 7-11, U(10)). Similar results are seen for swelling. A summary of the calculated results for channels 2 and 7 at the termination of SAS output is shown in Table 2.1.

The importance of looking at a radially varying release fraction and swelling is perhaps even more important for channel 2 than for channel 7. Figures 2.11 through 2.14 illustrate the channel 2 calculations. Release from node 2-11, 9 at initiation of slumping is 49.9% as compared to a single node calculational result of 30.4% and a mass-weighted average of 34.2%. Node 2-11, 10 has seen a release of only 5.69% at slumping initiation. The outer rind of fuel represented by node 2-11, 10 thus retains at initiation of slumping almost 95% of its original gas inventory. This retained gas represents over half of the gas still unreleased at axial node 11 even though the mass of fuel associated with radial node 10 is only half that associated with radial node 9.

The trends in gas behavior suggested by these calculations of LOF and TOP channels should be even stronger if a finer radial mesh is adopted. The implications of these trends to the resulting behavior of LOF and TOP channels would be as stated in the introduction and reiterated here.* Total releases and swelling before slumping (LOF) and pin failure (TOP) will be somewhat higher when a radially dependent calculation is performed than when the unrestructured fuel is treated as a single zone. The increased releases would in general decrease dispersion potential in the LOF accident while increasing driving forces for fuel ejection from the pin and possible fuel-gas-induced voiding in TOP channels. The distribution of gas remaining in the fuel for either situation would be weighted heavily toward the outermost areas of the unrestructured region.

---

*Note that the assumption of essentially unrestrained motion of intergranular gas (except where strong, intact cladding exists) is crucial to these implications.

TABLE 2.1

End Point Results for Various FISGAS3 Calculations

Run #	End Time (sec)	Gas Release (%)	Swelling (%)
7-11, 9	12.469	16.73	12.88
7-11, 10	12.469	1.49	5.49
7-11, U(10)	12.469	9.16	9.70
7-11, wtd. avg.	12.469	11.34	10.26
7-14, 8	12.469	14.56	13.08
7-14, 10	12.469	0.358	4.08
7-14, U(10)	12.469	6.65	8.75
2-11, 9	12.43	49.86	18.41
2-11, 10	12.43	5.69	7.44
2-11, U(10)	12.43	30.35	18.56
2-11, wtd. avg.	12.43	34.25	14.53
2-14, 8	12.43	28.49	19.06
2-14, 10	12.43	1.75	4.67
2-14, U(10)	12.43	18.29	13.81

The availability of the unreleased gas to contribute to fuel dispersal in the LOF channels should be limited; time scales for further release or availability should perhaps be estimated from heating rates at initiation of slumping. Immediate availability of a large fraction of this gas may be difficult to justify.

The effect of this earlier release and redistribution of gas on TOP channels should be less important. Less gas is available or accessible from the fuel following failure, but more gas is released to the central cavity at any time up to failure.

2.7 Comments on Validity of PFRAS

Since FRAS AND PFRAS were developed, a series of tests, FGR-32 through -36, conducted at Hanford Engineering Development Laboratory (HEDL) have been analyzed.[12] The results of these tests are in sharp disagreement with the corresponding FRAS/PFRAS analyses. (See Table 2.2)[13]. Several reasons for these discrepancies have been hypothesized.

One factor which might have contributed to the inaccuracy of the FRAS/PFRAS calculation is that the data base upon which parameters such as surface-diffusion coefficient and heat of transport were determined, was very limited. However, because of the large difference between experimental results and calculated values, other factors are probably contributing as well.

As mentioned earlier, the model used in the FRAS code assumes that the fuel grains can be approximated by spheres of some effective diameter. It was believed originally that any geometric factors could be compensated for by appropriate calibration of parameters such as the surface-diffusion coefficient. Recent analysis has shown this assumption to be incorrect[13].

Another simplification used in PFRAS which may lead to significant errors, is that bubble relaxation times are ignored[13]. Gruber's model assumes that bubbles instantaneously reach an equilibrium size after coalescense. Actually, after coalescense, volume is initially conserved. Volume diffusion then takes place, and after a finite time (i.e. relaxation time), the resultant bubble reaches its equilibrium size. The effect of including these relaxation times would be to reduce the bubble size distribution at any given time, thus increasing bubble mobility; the end result being an increase in gas release, and a decrease in swelling. This subject is presently being examined in greater depth at ANL and other places.

TABLE 2.2

Comparison of FRAS with Fission Gas Release Tests[12]

Test	FRAS Results		Measured Release (%)
	Swelling (%)	Release (%)	
FGR-32	330	9.5	97*
FGR-34	365	9.4	57
FGR-35	364	9.6	53
FGR-36	83	4.7	26

*The much higher measured release in this test may have resulted from overheating when the sample touched the capsule wall.

2.8 Summary and Conclusions

From the gas release results presented in Section 2.5, it is clear that a simple-radial-node representation of unrestructured fuel in transient gas release calculations can be misleading. A multi-nodal approach will likely predict larger overall releases during the transient and shows that the distribution of retained gas shifts strongly toward the outer rind of colder unrestructured fuel.

The implication of this behavior to LOF channels is two-fold. Less total gas is present in the fuel at initiation of slumping, and the gas that is present may not be readily available to act as a dispersing force.

The implication to TOP channels is a larger released gas inventory at failure with resulting greater fuel ejection rates and potential for direct fuel-gas-induced voiding in the LOF-Driven-TOP.

It is important to point out again that the conclusions stated above are based on the assumption that gas is free to move through existing interconnected porosity once the gas reaches a grain boundary.

SECTION 2 REFERENCES

1. E. E. Gruber, "Calculation of Transient Fission Gas Release from Oxide Fuels," ANL-8143, Argonne National Laboratory (November 1974).

2. E. E. Gruber, "Fission Gas Behavior," ANL-RDP-37, Argonne National Laboratory, 7.5 (February 1975).

3. E. E. Gruber, "Fission Gas Behavior," ANL-RDP-39, Argonne National Laboratory, 7.15 (April 1975).

4. E. E. Gruber, "A Generalized Parametric Model for Transient Gas Release and Swelling in Oxide Fuels," Submitted for Publication to the Journal of Nuclear Technology (1977).

5. J. F. Meyer, et al., "An Analysis and Evaluation of the Clinch River Breeder Reactor Core Disruptive Accident Energetics," NUREG-0122 (March 1977).

6. L. W. Deitrich, et al., "Modeling the Response of Fast Reactor Fuel to Accident Transients," Proc. of Int. Mtg. on Fast Reactor Safety and Related Physics, CONF-761001, Vol. IV, p. 1715 (October 1976).

7. J. Crank, The Mathematics of Diffusion, Oxford University Press, London, Great Britain, 86 (1956).

8. A. H. Booth, AECL-496 (September 1957).

9. P. L. Garner, "DIFFSYS," University of Virginia (July 1972).

10. R. Bulirsh and J. Stoer, "Numerical Treatment of Ordinary Differential Equations by Extrapolation Methods," Numerische Mathematik, 8, 1-13 (1966).

11. P. L. Garner, "DIFFDRV," University of Virginia (July 1972).

12. "HEDL Technical Progress Report, Semi-annual, January-June 1975," HEDL-TME-75-72, Hanford Engineering Development Laboratory (1975).

13. E. E. Gruber, "FRAS Code Development," ANL-RDP-54, Argonne National Laboratory, 6.48 (September 1976).

3. TREAT EXPERIMENT MODELING

3.1 Previously Reported Work

We have been interested in analyzing TREAT experiments related to the transient overpower accident for two primary types of reasons as outlined in Reference 1. First we were looking for rather general results concerning possible operative phenomena, e.g., whether the observed experiment results are explainable in terms of fuel-coolant-interactions (FCI), and whether flow blockages might be expected under observed voiding and fuel motion patterns. Second, we were interested in applying to experiment analysis the simple models we have used in analysis of voiding in subassembly geometry[1,2,3].

Our first attempt at analysis of a flowing sodium experiment was reported in a previous topical[1]. The H2 experiment[4,5] was selected for analysis because it had been analyzed previously by others, and a relatively large amount of information on the test was available. Also H2 was a single pin test, which should, therefore, make it more amenable to analysis by single pin codes such as our UVAFCI Code[2].

Our H2 analysis followed the lead of Cronenberg[6] in many respects. Calculations were started approximately 40 ms after first indications of possible pin failure. The FCI zone contained two-phase sodium at that time. Whether the pin really failed at the time assumed by Cronenberg or simply experienced a 40 ms period of per-failure boiling is not clear.

Our efforts at modeling H2 were marginally successful. The voiding histories we calculated were shifted upward significantly from experiment results. This is shown in Figure 3.1, which is reproduced from Reference 1. In addition to the experiment results and our UVAFCI calculations, the results of a calculation from Reference 6 is shown in the figure. The Case I results were chosen for comparison because initial conditions for the Case I calculation and our UVAFCI calculation

were very similar. As indicated in Reference 1, we feel that the upward shift in our calculated voiding pattern relative to the experiment is due to our inability to model formation of a partial blockage which probably began within some 60 ms after pin failure (20 ms after time zero in Figure 3.1).

We also discussed in Reference 1 the reasons why the 5g of molten fuel considered in the H2 analysis gave a relatively weak interaction compared to what we have calculated for subassembly geometries in which 5g of ejected molten fuel per pin was modeled. Several factors were brought up, including heat loss rates from the FCI zone, total heat sink available, ejected fuel temperatures, etc. However we suggested that the most important factor was the high void fraction present at all times in the FCI zone in the H2 analysis. Single-phase pressures never developed, and fuel-to-sodium heat transfer was impeded at all times by the presence of sodium vapor.

The early development of such large sodium void fractions may not be so easy under CRBR conditions. The smaller sodium inertia and pump head available in TREAT tests relative to prototypic subassembly geometry may permit rapid FCI zone expansion before significant fuel fragmentation and mixing and associated strong heating of the sodium has occurred. Such would not be the case in subassembly geometry under full flow conditions. This would especially be important in the failure of irradiated pins. Relatively small amounts of gas could initiate significant voiding in TREAT loops compared to required gas releases under CRBR conditions.

The interest in looking at irradiated pin plus giving consideration to multiple rather than single pin geometries were factors in our decision to look at the H5 test as a followup to the H2 work.

3.2 Seven-Pin Test Geometry

The move from a single pin test simulation (H2) to a seven-pin test simulation raised again the question of two dimensional (2D) versus one dimensional analysis of the FCI zone. Certainly the non-uniform flux distribution in the multiple pin TREAT tests[4] would lead

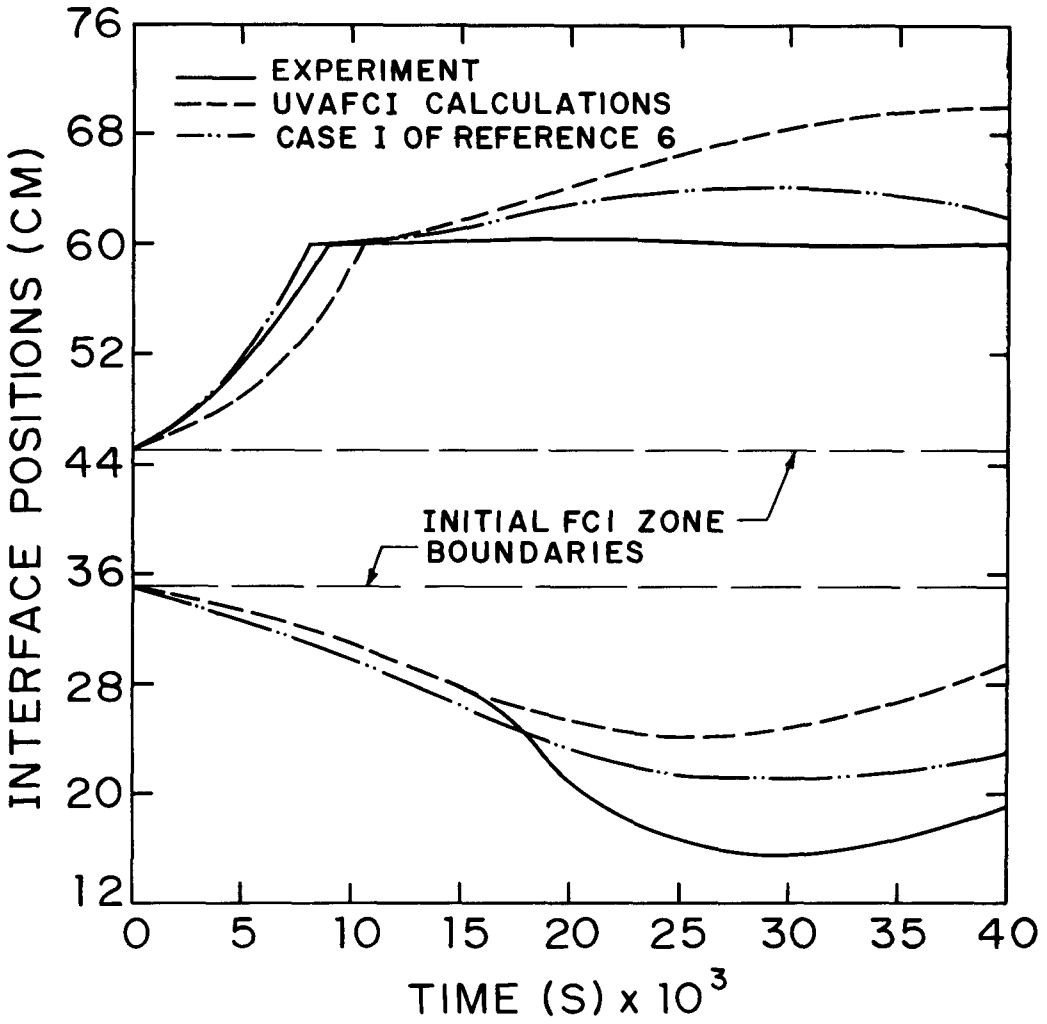

Figure 3.1 UVAFCI Calculation of H2 Voiding Compared with Experiment Results and with Previous Calculations by Cronenberg[6].

to non-coherent pin failure even if all the pins in a given test were identical. In tests like H5[4] the difference in pins is truly significant with only one irradiated pin present, surrounded by fresh pins. (In H5 the pin characteristics offset the non-uniform flux distribution completely, and the central, irradiated pin appeared to fail first).

Arguments can be made that 2D effects in voiding are more important in 7-pin tests than under CRBR conditions. This might especially be true with the mild interactions such as H5 appeared to experience following failure of the central irradiated pin. For vigorous voiding, the 2D effects should be less important. As in previous work[2] we have confined ourselves in 7-pin analyses to selection of appropriate sodium masses and available heat loss surfaces when considering possible 2D effects.

Several interesting aspects of looking at single-pin-failure in a 7-pin test are worth discussing here. The area per centimeter length of test section available for heat losses from the FCI zone is 23.7 cm^2 compared to 2.3 cm^2/pin/centimeter length in subassembly geometry. Also the mass of steel heat sink available per centimeter length of test section is 10.3 g versus about 1.09 g/pin/centimeter length in subassembly geometry. These considerations tell us that, if the FCI zone does indeed spread radially on a short time scale compared to the interval between first and second failures in a 7-pin test, the interaction will likely be a very mild one. Secondary failures must occur rapidly in order to generate strong interactions. This is consistent with observed test results.

In setting up the hydraulics model for H5 geometry we followed the same general procedure that we had for H2. Pressure drops due to friction and to losses at area changes were modeled as was the loop plenum pressurization during test section voiding. A steady state run was made to insure proper flow rates. In retrospect we find that our choice of pump characteristics was probably not good. They resulted in zero flow pump head of about two-thirds of an atmosphere

rather than a one atmosphere head as used by Sonnichsen, et al.[7]. The 5 psi difference would probably not be a big factor in characterization of resulting voiding patterns for vigorous FCI's (as modeled, for example, in Section 3.4), but could be important in some of the milder voiding results discussed in the next section, Section 3.3.

3.3 Analysis of H5

The initial conditions for the UVAFCI run which we made in an attempt to reproduce results of the first pin failure in H5 were taken from various reports, including References 4 and 7. The central irradiated pin was apparently the first to fail, with an interval in excess of 25 ms between the first and second failures. We assumed that a total of 1 g of molten fuel at a temperature of 3100 K (fuel at the liquidus might have been a better choice) was injected into the interaction zone over a period of 9 ms. The fuel was modeled as spheres of 100 μm radius. Initial sodium temperature was taken as 978°C, and a total sodium mass of 6.0 g was involved in the interaction.

The highest pressures observed in the experiment were the order of 100 psia, but pressures on the cladding I.D. at failure would probably be the order of 100 atm or more. Therefore, an initial interaction zone pressure of 15 atm was arbitrarily selected so that ejected fission gas would not occupy an unrealistically large volume at time zero. A fission gas mass of 1 mg was assumed for the calculation. It turned out that these assumptions on initial pressure and mass of gas in the interaction zone are crucial for such a mild interaction. Consider various values of initial pressure and mass of gas (initial temperature 3100 K) as shown in Table 3.1 below and the corresponding final volume occupied by the gas at 2.8 atm (steady state pressure at the failure site). The total outlet flow volume in H5 in the first 10 ms after failure was only $\sim$ 8.5 cc[7], and normal flow rates would account for $\sim$ 7 cc of this flow volume. Thus it is

TABLE 3.1

Isentropic Expansion Results for Monatomic Ideal Gas

Mass of Gas (mg)	Initial Pressure (atm)	Volume at 2.8 atm (cc)	Work Done to 2.8 atm (Joules)
1	15	.387	.263
1	100	.181	.408
5	15	1.934	1.313
5	100	.906	2.042

clear from the above table that uncertainties in the mass, temperature and initial pressure of gas introduced into the sodium at and soon after pin failure could account for experiment flow data between the first and second pin failures. (Using the initial conditions outlined at the beginning of this section, the corresponding flow volume we calculated with UVAFCI during the 10 ms interval of interest was 7.7 cc).

Our UVAFCI mockup of the H5 initial pin failure assumed that the initial void fraction was due entirely to the fission gas expelled from the pin. The pressure history was dominated by the pressure of this gas, with the peak calculated pressure being essentially the initial pressure of 15 atm. No sodium vapor was produced. The 1 g of fuel ejected from the pin was simply quenched by the sodium.

The total energy given up by the fuel to the sodium in the first 10 ms following failure was almost 1300 J, but spread over 6 g of sodium, this results in only 1200°C sodium when heat losses to structure are also factored in. The work done on the constraining sodium columns was thus due almost entirely to fission gas expansion and had a value less than 1 J, consistent with Table 3.1 work numbers.

Our calculation was, of course, parametric, and the use of different masses of sodium would give different results. The 6 g amount was based on full sodium flow for 10 ms. The exact amounts of sodium and fuel (fragmented or unfragmented) involved in the FCI at any time following failure is impossible to determine. However, our calculations plus the above discussion suggests that if the initial pin failure resulted in ejection of only the order of 1 g of fuel during the interval up to second pin failure, the pressure and voiding histories were probably dominated by ejected fission gas.

We felt it would be worthwhile to examine the behavior of an H5 type of initial failure in which much larger amounts of fuel would be ejected from the initially failing central pin. We selected a

total of 9.6 g of fuel to be injected over a 10 ms period consistent with our previous work[2]. Other parameters which differed from the original H5 mockup were fuel particle diameters (increased from 200 to 632 μm), initial fuel temperature (increased from 3100 to 3200 K), fission gas released (increased from 1 to 9.6 mg, consistent with the increase in fuel mass), and sodium-to-cladding heat loss coefficient (decreased from 1.356 to 0.452 cal/cm^2•s).

The calculated voiding history for the 120 ms following failure is shown in Figure 3.2. Several points should be noted. Sodium vaporization first began at about 5.5 ms into the calculation. Voiding to that point was once again due primarily to the fission gas. The FCI zone oscillated in size with a period of about 35 ms, which seems to be characteristic of the test loop. (Other cases discussed below gave similar periods of oscillation). The zone oscillations were centered near the initial zone/failure location. If the presence of large void fractions at the ejection site is a contributing factor to blockage formation as we have often suggested, the potential is clear for blockage formation near the failure site for this strength of interaction in the 7-pin loop geometry. This point will be addressed further in Section 3.4, including its application to more prototypic subassembly geometry.

3.4 Investigation of More Energetic FCI's in H5 Geometry

The calculational results discussed in Section 3.3 provided information as to what might be expected for single pin failures resulting in 1 to 10 g of fuel ejected over a 10 ms period. However, we were also interested in comparing the pressurization and voiding results which would be obtained in the H5 geometry to that obtained in CRBR subassembly geometry for comparable strength FCI's.

The subassembly case selected for comparison was designated BURN850C and is described in Section 5.3 in some detail. It represented a very mild case relative to other subassembly cases examined previously[2]. The average amount of molten fuel ejected per pin was

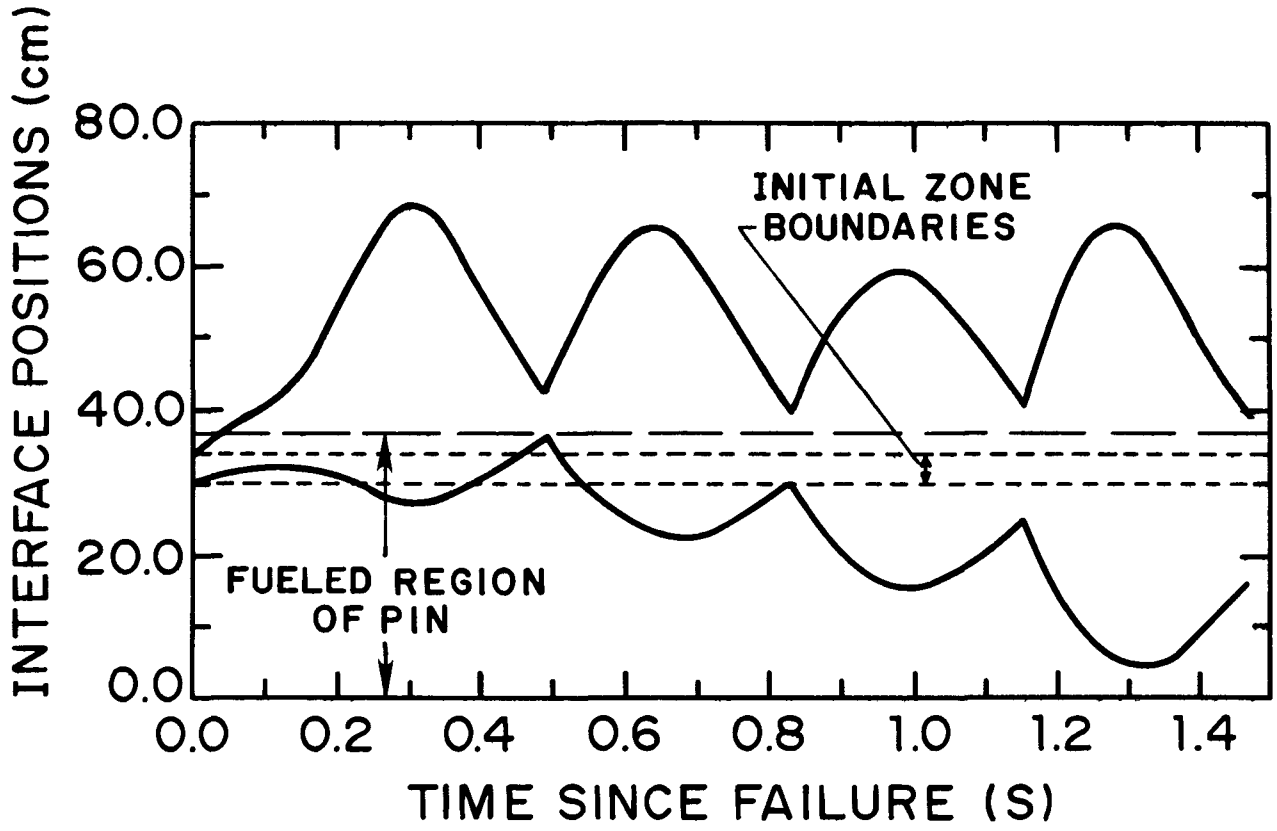

Figure 3.2 Calculated Voiding History for Ejection of 9.6 g of Fuel Following Single-Pin-Failure in H5 Geometry.

4.8 g; this ejection took place over quite an extended period (50 ms). These and other important parameters are listed in Section 5.3.

Having selected BURN850C, we set up the equivalent case in H5 geometry. A total of 33.6 g of molten fuel was considered for the 7-pin geometry. Fuel temperatures, particle sizes, etc. were the same as for BURN850C. The voiding histories for BURN850C (labeled CRBR geometry) and for the case in H5 geometry are shown in Figure 3.3.

It is important to emphasize that the UVAFCI slug model used in both of these calculations really has limited validity unless lower slug reversal occurs quickly. However, we can compensate for this to some extent by adjustment of sodium masses involved in the calculations.

Note that flow reversal in the case with CRBR geometry did not occur until about 40 ms after pin failure. With H5 geometry the first reversal occurred about 14 ms after initiation of the FCI. This difference is easily explainable in terms of the ratio of lower sodium column inertial lengths involved ($\sim$ factor of two larger for CRBR) and the initial sodium velocities (again almost a factor of two greater for the prototypic CRBR conditions).

Also note that, although the H5 geometry leads to more rapid initial void development, the ultimate void growth is limited by the Mark-IIA loop geometry with its relatively small volume for accommodation of sodium driven from the test section. Thus the axial center of the interaction zone never moves far from the failure site in H5 geometry, while in CRBR geometry, for this relatively weak FCI, the motion of the axial center of the FCI zone is predominantly upward at all times after failure. This difference in void pattern development would suggest that blockages such as that observed in the H5 test would be expected to form near the failure site in H5 geometry even for relatively mild FCI's (if significant fuel enters the coolant channel after void initiation), while such blockages might not be so likely to form in CRBR geometry.

Once again we see in the case with H5 geometry an oscillatory voiding behavior similar to that seen in Figure 3.2. The period of oscillation again is the order of 35 ms. Such behavior would only be observed in experiments if no blockages formed.

3.5 Summary

Our efforts to model TREAT fuel dynamics tests performed in flowing sodium loops have accomplished several things. We have gained confidence in the computer models previously used for modeling FCI's in subassembly geometry. We have seen the relative ease of voiding initiation in the TREAT Mark-IIA loop compared to CRBR geometry. Moreover, we have also seen that voided regions appear less mobile in the Mark-IIA loop. These two behavioral patterns do indeed suggest that the formation of blockages, under a given driving force for voiding, would be easier in the Mark-IIA loop than in CRBR geometry. This conclusion is based on our previously stated contention that the major factors favoring blockage development are the creation and long-term existance of high void fraction regions at the failure site.

Note, however, that in multiple-pin TREAT tests the initial pin failures generally result in little void formation and that secondary failures are needed to set up the conditions favorable to blockage formation. This is consistent with our various TREAT and CRBR calculations for lower (~.2g/ms/failed pin) fuel ejection rates, i.e. with the low rates, near-simultaneous failure of a large fraction of the pins is required to produce significant voiding.

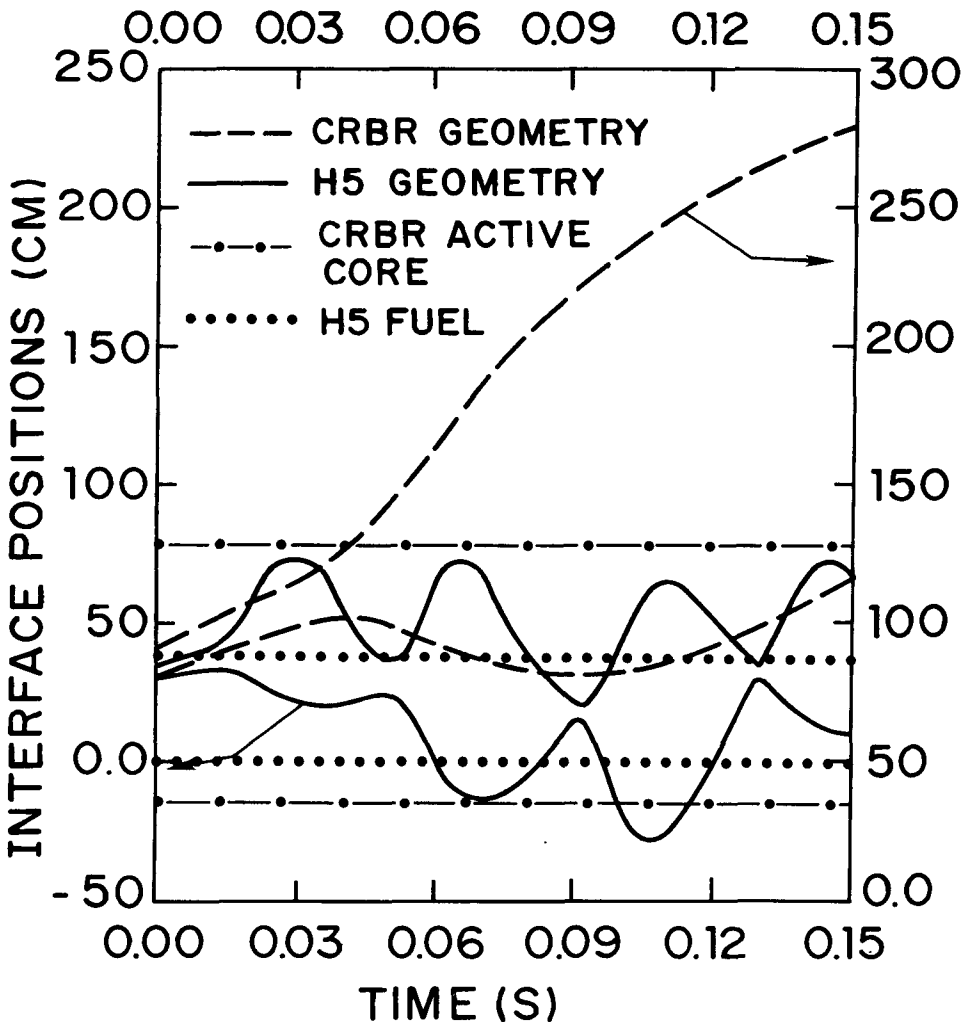

Figure 3.3 Comparison of Equivalent FCI's in CRBR and H5 Geometry, Illustrating the Effect of the Closed Loop for the H5 Geometry.

SECTION 3 REFERENCES

1. C. A. Erdman and M. B. Johnson, "Some Aspects of Subassembly Voiding in the Unprotected Transient Overpower Accident in LMFBR's," NUREG-0277 (June 1977).

2. University of Virginia, Annual Report for the Period July 1, 1975-June 30, 1976, NRC Contract No. AT(49-24)-0158.

3. C. A. Erdman and M. B. Johnson, "Some Aspects of Fuel Motion in the Unprotected Transient Overpower Accident in LMFBR's," NUREG-0282 (June 1977).

4. A. B. Rothman et al., "Review of TREAT Experiments in Support of Transient Overpower (TOP) Analysis for Fast Reactor Safety," Proc. of the Fast Reactor Safety Meeting, Beverly Hills, California, CONF-740401-P1, pp. 205-219 (April 1974).

5. A. B. Rothman et al., "Failure Threshold TREAT Experiment with an Unirradiated Prototypical FFTF Fuel Element, Trans Am. Nucl. Soc., 13, 652 (1970).

6. A. W. Cronenberg, "A thermodynamic Model for Molten UO_2-Na Interaction Pertaining to Fast-Reactor Fuel-Failure Accidents," ANL-7947 (June 1972).

7. J. C. Sonnichsen et al., "Analytic Modeling of the Mark-IIA TREAT Loop for Fuel Motion and Sodium Expulsion Studies," Loc. Cit. 4, pp. 220-238.

4. REVIEW OF ANL UPPER PLENUM INJECTION TESTS

4.1 Introduction

One of our tasks for FY77 was the investigation of the likelihood of the occurrence of plenum pressurization in LMFBR accidents. By plenum pressurization we mean here the generation of large overpressures following the ejection of molten or two-phase core materials into the gas plenum region of an LMFBR. The hypothesized pressurization mechanism would be the vaporization of sodium originally present in the plenum region.

We decided to execute this investigation in two parts: a review of experiment programs at ANL[1] and a development of analytic capability for predicting the pressurization. This section of the report concentrates on the ANL experiments. Reference 1 has been utilized as the prime source of information on these experiments.

Apparently the intent of one or two of these experiments was to promote molten fuel/sodium mixing via the injection of molten fuel into a pin bundle containing sodium. However, as will become evident later in this section, the void fractions associated with the injected material were such as to more properly represent the injection of hot non-condensable gases into sodium regions. The nature and extent of fuel/sodium contact in the tests is not clear.

The three tests mentioned in Reference 1 had different amounts of sodium present in the pin bundle. In test UPI No. 1, the pin bundle was half full; UPI No. 2 utilized an empty bundle; UPI No. 3 had a completely full bundle. UPI No. 3 was not discussed to any great extent in Reference 1. No further information on UPI No. 3 has been published. Various aspects of the tests as described in Reference 1 will be addressed in the following sections of this report.

4.2 Thermodynamic Calculation of Thermite Temperature

Using the stoichiometry indicated in Table I of Reference 1, we calculated the adiabatic flame temperature of the thermite reaction mixture to be 3800°K; this is in fair agreement with the calculated and measured value of 3470°K at the throat of the thermite injector reported in Reference 1. Thus, it is reasonable to conclude that the thermite reaction went essentially to completion and that the composition of the injected two-phase fluid is accurately represented in Table I of that report.

4.3 Conditions of the Injected Thermite Mixture, UPI No. 1

Reference 1 indicates via its Table I and Figure 6 that the initial void fraction of the thermite reaction mixture was 0.75. However, we find this value inconsistent with other data presented in the report. To be specific, note that the mass ratio of the liquid and gas phases in the injector may be related by α according to the equation:

$$\frac{m_{liq}}{m_{gas}} = \frac{\rho_{liq}}{\rho_{gas}} \left(\frac{1 - \alpha}{\alpha} \right)$$

Assuming that the density of the liquid phase in the thermite reaction mixture is 9g/cc (Reference 1 apparently used 9.96 g/cc) and that the gas density is close to 0.00484 g/cc (750 psi, 3800 K), these density values combine with the reported values of $\alpha = 0.75$ to yield a mass ratio of 620. However the actual mass ratio in the reaction mixture was only 114 (i.e., 683 g of liquid ÷ ∿ 6 g of gas). It seems, therefore, that the reported value of $\alpha = 0.75$ is too small.

Using the above phase densities and the reported phase masses (as obtained from Table I of Reference 1), we determined the corresponding value of the void fraction for the thermite reaction mixture to be $\alpha = 0.94$. Thus, the injected thermite mixture was more "gas-like" in its properties than indicated in Reference 1.

The injector throat flow conditions and the downstream flow conditions were checked by treating the injection mixture as a pseudo-gas (as outlined by G.B. Wallis[2]). Two different models were considered, one involving no heat transfer between the phases, the other taking the two phases to be in thermal equilibrium. The results are presented in the following table (Table 4.1), which also includes the corresponding calculated values from Reference 1. Considering the conditions at the throat and downstream of the throat, there is fair agreement between us and Reference 1 with regard to the void coefficient, but not with regard to $(1 - \alpha)$, and only order-of-magnitude agreement with regard to the calculated fluid velocities. (It should be noted that Reference 1 obtains the downstream velocity by application of an approximate form of the Bernoulli equation, which is of dubious validity in this compressible flow situation.)

Neither our calculated fluid velocities nor the Reference 1 calculated fluid velocity agree with the experimentally observed UO_2 velocity, estimated to be about 40m/s from the data in Figure 5 of Reference 1. However, in view of the high void fraction of the injection mixture and the manner in which the UO_2 fuel velocity was determined, we feel that the experimental value of 40 m/s may markedly underestimate the velocity of the injected mixture at impact.

4.4 Impact Calculations, UPI No. 1

Using the pseudo-gas models suggested by Wallis[2], the impact pressures at the sodium interface were estimated to be between 2.5 and 21.2 MPa. These calculated values show an order-of-magnitude agreement with the experimental value of 6.9 MPa. Thus we agree with Reference 1 that the measured value is indeed possible and probable in the system studied. However, in a more realistic situation, involving the injection of molten UO_2 with a void coefficient considerably less than 0.98, a much greater impact pressure could be expected. Subsequent phenomena could also vary considerably from those observed in the experiment.

TABLE 4.1

Injector Throat and Downstream Flow Condition, UPI No. 1

Model	Throat			Downstream		
	P (MPa)	V(m/s)	α	P (MPa)	V(m/s)	α
pseudo-gas no heat transfer	2.69	43	0.966	0.1	115	>.98
pesudo-gas thermal equilibrium	3.08	36.6	0.961	0.1	275	>.99
Reference 1	2.1	48	0.85	0.1	75	0.98

Figure 7 of Reference 1 shows the time-dependence of the gas plenum pressure, and indicates a peak value of about 0.3×10^6 Pa (3 atm). Assuming isentropic compression of the gas and an initial volume indicated on page 1739 of Reference 1, we calculated a value of 58.5 joules of work done on the gas as it was pressurized to its peak value. The Reference 1 value of 180 joules is apparently wrong. However, the conclusion remains the same, namely, that the sodium absorbed only a small fraction of the total initial kinetic energy of the injected fluid. It is interesting to note that at the time of maximum gas pressurization to 3 atm, only a small fraction of the total reactant product mass could have given up kinetic energy to the sodium column. Based on Figures 6 and 7 of Reference 1, less than 20% of the reactants would even have left the injector. It is not clear that the total work done on the plenum gas up to that time could be accounted for by the kinetic energy of the fuel ejected up to that time. If our Table 4.1 "throat" results were assumed true, the discrepancy would be even greater. Indeed, for the conditions of Table 4.1, there is no way the work done on the plenum gas (even neglecting frictional losses in the sodium) could be accounted for by ejected material kinetic energy.

The experimental data for UPI No. 1 indicate a second impact pressure approximately 10-11 msec into the transient. Other than attributing it to a "second impact", the report offers no further analysis. This is somewhat surprising, since the magnitude of the second impact pressure is as large, if not larger, than the initial impact pressure (see Figure 4, of Reference 1).

4.5 Sodium Film on Pins in UPI No. 1

Reference 1 does not specifically discuss the magnitude of the sodium films remaining in the region which had been drained of sodium prior to injection of thermite reaction products in UPI No. 1. However, earlier preliminary documentation indicated an elapsed time

in excess of 10 sec. between completion of draining and initiation of injection.

Using the analysis of Bird, Stewart and Lightfoot[3], we estimated the film thickness by the following relationship:

$$\delta = \sqrt{\frac{\mu z}{\rho g t}}$$

The mass of the film per pin may be determined from:

$$m = \int_0^z \pi D \delta \rho \, dZ = \frac{2}{3} \pi D \rho \delta Z$$

Substituting Z = 0.15 m, t = 10 s, $\gamma = 2.5 \times 10$ m^2/s, D = 5.84×10^{-3} m, ρ = 800 kg/m^3 and g = 9.8 m/s^2 yields a film mass of 2.87×10^{-5} kg per pin and a total film mass of about 1.06 g for the 37-pin assembly. A rough estimate was made to check on the pressure that could be developed by vaporization of this mass of sodium if it were allowed to instantaneously equilibrate with the associated injected mixture up to time of impact.

Assuming a volume of 111 cc available to the sodium vapor (based on flow area external to the pins over a 15 cm length of the pin bundle), pressures of the same order of magnitude as the proposed impact pressures can be calculated. This statement is based on equilibration of 21 g of UO_2 initially at 3400 K with 1 g of sodium initially at 920 K.

Only about 4000 J is needed to convert that sodium to saturated vapor at 1 atm. This amount of energy would just about lower the fuel to its liquidus. The large heat of fusion of the fuel would insure that the resulting equilibrium temperature would be about 3040 K. This would translate to a sodium pressure of about 98 atm or 9.8 MPa. If losses to cladding dropped sodium vapor temperature to the range of 2150 K or if an additional 50 cc of volume were available above the pin bundle, the resulting sodium pressure would be right at the initial measured pulse value of 6.9 MPa.

We are not claiming that such a vaporization process caused the initial pressure pulse. The pulse width seems much too small for such to be the case. Also the time scale available for thermal equilibration would seem too short. However, it is useful to investigate alternate scenarios, if for no other reason than to ascertain their relative probability. Note that further sodium/fuel mixing following voiding of the pin bundle would likely introduce a quenching effect initially because of the large amounts of sodium added compared to the smeared fuel density in the expanding thermite mixture. Each centimeter of newly exposed sodium film would introduce the order of 0.85 g of sodium.

4.6 Physical Examinations of Test Assemblies

The conclusions drawn in Reference 1 concerning the disposition of the injected mixture and the role of the sodium coolant appear to be reasonable for both UPI No. 1 and No. 2.

4.7 Summary of Review

It seems likely that sodium vaporization was not a primary pressurization source in the ANL upper plenum injection tests. However, the thermite mixture provided source conditions of such large void fractions that nothing definitive can be shown regarding the likelihood of pressurization in a reactor-type situation.

The simulant fluid experiments mentioned at the end of Reference 1 may provide a better simulation of void fractions and flow regimes; however, a better experiment (i.e., with regard to source conditions) using reactor materials is also needed.

SECTION 4 REFERENCES

1. R. E. Henry et al., "Experiments on Pressure-Driven Fuel Composition with Reactor Materials," Int. Mtg. on Fast Reactor Safety and Related Fields, CONF-761001, Vol. IV, p. 1734 (October 1976).

2. G. B. Wallis, One-Dimensional Two-Phase Flow, McGraw-Hill, N. Y., p. 20ff (1969).

3. R. B. Bird, W. E. Stewart, and E. N. Lightfoot, Transport Phenomena, John Wiley and Sons, Inc., N. Y., p. 69 (1960).

5. REVIEW OF OTHER FY77 WORK

5.1 Introduction

In addition to monthly letter reports, the topical reports[1,2], and the final report which were specifically defined in our Scope of Work for FY77, several other pieces of written material were supplied to DPM this past year. This material included a writeup on the LOF-Driven-TOP, originally submitted July 1976, and a response to a January 10, 1977 request for implementation of action items generated at the December meeting on fission gas as a fuel dispersing mechanism.

Other consulting activities included attendance at the various meetings listed below:

(1) 9/8/76 meeting at Bethesda on pin failure

(2) 9/22/76 meeting at Bethesda for presentation by ANL staff on CRBR CDA energetics

(3) 9/29/76 meeting of ACRS Subcommittee on CDA energetics at Oak Ridge, Tennessee

(4) 10/5-8/76 meeting on fast reactor safety in Chicago, Ill.

(5) 12/9/76 meeting at Bethesda on fission gas as a dispersal mechanism

(6) 1/26,27/77 meeting on LOF at ANL

(7) 3/3/77 meeting at Bethesda on SAS3D

(8) Meetings at Bethesda and Charlottesville to update DPM staff on contract progress (last meeting on 9/30/77).

Specific requests were received from DPM personnel for consultation on and verbal or written response to several other technical items during the past year not mentioned above. These items included a review of sections of the FFTF FSAR, consideration of CDA work calculations as a function of the assumed equation of state, review of recent analyses showing sharp reductions in CDA work over earlier predictions, and consideration of various thermodynamics and thermal

ydraulics questions encountered by DPM staff. Some additional contract work not mentioned in the above paragraphs or treated in previous sections of this report is addressed in the remaining parts of this section.

5.2 Topical Reports on Fuel Motion and Subassembly Voiding

References have already been made in this report (Section 3.1) to topicals[1,2] released in FY77. Here we will summarize the results and conclusions of those topicals. The reports on fuel motion[1] and subassembly voiding[2] both dealt primarily with extensions of our FY76 work areas. Let us first discuss the fuel motion report.

The question of fuel expulsion dynamics in the classical TOP was addressed. In particular, the significant delay time observed experimentally between irradiated pin failure and ejection of significant amounts of fuel into the channel was discussed. We indicated that fresh pins might be expected to have a shorter delay time but that the R9 test[3] seemed to contradict the shorter delay time hypothesis. Since releasing the report we have found that the delay time in R9 may have really been quite short (consistent with the original hypothesis) and that problems with the neutron nodescope data interpretation may have been responsible for initial reporting of a long delay time[4]. At this point then, use of the easy access model (e.g. in PLUTO[5] and EPIC[6]) for ejection of molten fuel immediately following failure of irradiated pins does not really seem justifiable.

Once fuel does enter the coolant channel, there would seem to be, at first glance, sufficient forces to easily remove fuel from the core region. However, a relatively small impulse ($\sim$ .01 MPa•S) is sufficient to stop full coolant flow in CRBR, and a longer term overpressure of only 0.8 MPa would establish and maintain downward voiding. An efficient FCI involving a few grams of fuel per pin could accomplish this. Plenum gas releases probably could not.

If flow perturbation and resulting large void fractions at the failure are established, the fuel subsequently ejected from the pin and into the void is less likely to fragment via thermal fragmentation mechanisms. This fuel then has the potential for initiation of flow blockages, as observed so often in the TREAT flowing sodium tests. Our conclusions were as follows:

- general upward dispersal will be effected initially
- partial or complete blockages are likely due to fuel or fuel/steel freezing, but the location and timing of these blockages is still in question
- significant early voiding probably enhances development of blockages.

Both the fuel motion and subassembly voiding reports addressed in part various aspects of the LOF-Driven-TOP accident. Our concern had been directed to the possibility of rapid, extensive sodium voiding in the TOP channels without compensating fuel motion. One possible source of such voiding is plenum gas release. Certainly the reduced pump head and sodium flow in the LOF accident relative to the classical TOP would seem to make the voiding more important in the LOF-Driven-TOP; however, our analysis of the LOF-Driven-TOP plenum gas releases indicated that the associated reactivity insertion rates were insignificant, even without consideration of non-coherence effects.

Other potential means of voiding in the LOF-D-TOP are an FCI or direct fuel-gas pressurization. The key to determining the importance or operability of either mechanism is a definition of the degree of communication between the coolant channel and pin interior and of the energy and momentum coupling between the ejected fuel and sodium in the coolant channels. We argued that opposite extremes of communication and coupling could result in large reactivity insertion rates for the first 10 to 20 ms following pin failure. Good energy coupling could produce a vigorous FCI utilizing only a small mass of fuel per pin (e.g., 2 g). The resulting rapid sodium voiding would introduce positive reactivity that far overpowers the associated fuel motion

reactivity. On the other hand, poor coupling would result in rapid sodium voiding due directly to the expansion of fuel gas in situations where good communication exists between the pin interior and the coolant channel.

We concluded that the possibility of rapid sodium voiding in the LOF-Driven-TOP accident with little compensating voiding cannot be ruled out for the period immediately following pin failure.

For a review of the work on TREAT test analyses reported in the topical on subassembly voiding, see Section 3 of this paper.

5.3 Importance of Fuel Ejection Rates

Our annual report[7] for FY76 contained rather extensive studies of the minimum requirements on FCI's for producing extended (both in time and space) voiding in subassembly geometry for the classical TOP. The interest in voiding was tied to the belief mentioned above that extensive voiding is a big factor in blockage formation.

The fuel ejection rates used in Reference 7 for failed pins were fairly high, e.g., 1g/ms for the first few milliseconds following failure. These rates were based on calculations made using the PLUTO and EPIC codes, which assume perfect communication between the pin cavity and the coolant channel at the failure site. However, depending on the mode and timing of failure, significant resistance to flow of molten fuel from the pin may occur between the pin cavity and the coolant channel. Small-area ruptures (e.g. crack-type fractures) can operate in conjunction with large pieces of solid fuel directly behind the cladding failure to provide strong local resistance to molten fuel motion. This could especially be important at failure sites where the pin cavity volume is small (e.g. well above the axial midplane).

The result of these local resistances could be lower rates of ejection of fuel into the coolant channel. The likelihood of the lower ejection rates and the effect of such lower rates on subassembly voiding were discussed with A. E. Waltar, visiting Associate Professor

of Nuclear Engineering during the 1976-77 academic year. Out of those discussions came an effort to look at the effect of reducing fuel ejection rates by a factor of five (to 0.2g/ms/failed pin) for some of the cases originally considered in Reference 7. The factor-of-five reduction was arbitrary and will be not justified explicitly.

First a very vigorous case labeled BURN5H from Reference 7 was considered in looking at the reduced ejection rates. We originally thought that the factor-of-five reduction might turn BURN5 into a rather benign case. This turned out not to be true. Details of the UVAFCI code input for the BURN5H case are given below.

- coherent failure of all pins
- 9.6g of molten fuel/pin into sodium over 9.5 ms period
- fuel particle size: 200 μm
- initial fuel temperature: 3500 K
- mass of sodium: 1.6g
- initial sodium temperature: 1000 K
- initial heat sink temperature: 1100 K

The case which modeled the reduced fuel ejection rate was labeled BURN5H50. Its input differed from that of BURN5H only in that the 9.6g of fuel/pin was introduced over a period of 45 ms (i.e. 0.21 g/ms/pin). Voiding histories for the two cases are shown in Figure 5.1 for comparison. There is indeed a significant reduction in the strength of the voiding, especially during the first 80 ms following initiation of the FCI. For BURN5H the lower zone interface went below the lower shield region for a significant period of time, and the upper zone interface exited the subassembly rather quickly.

The reduction in voiding strength for BURN5H50, although quite noticeable from Figure 5.1, was not as great as we had originally anticipated. The entire active core was still exposed to a high void fraction environment for over 75 ms. The initial rupture site was never recovered by the returning lower slug during the 120 ms run. The overall effect of reducing the fuel ejection rate was similar to

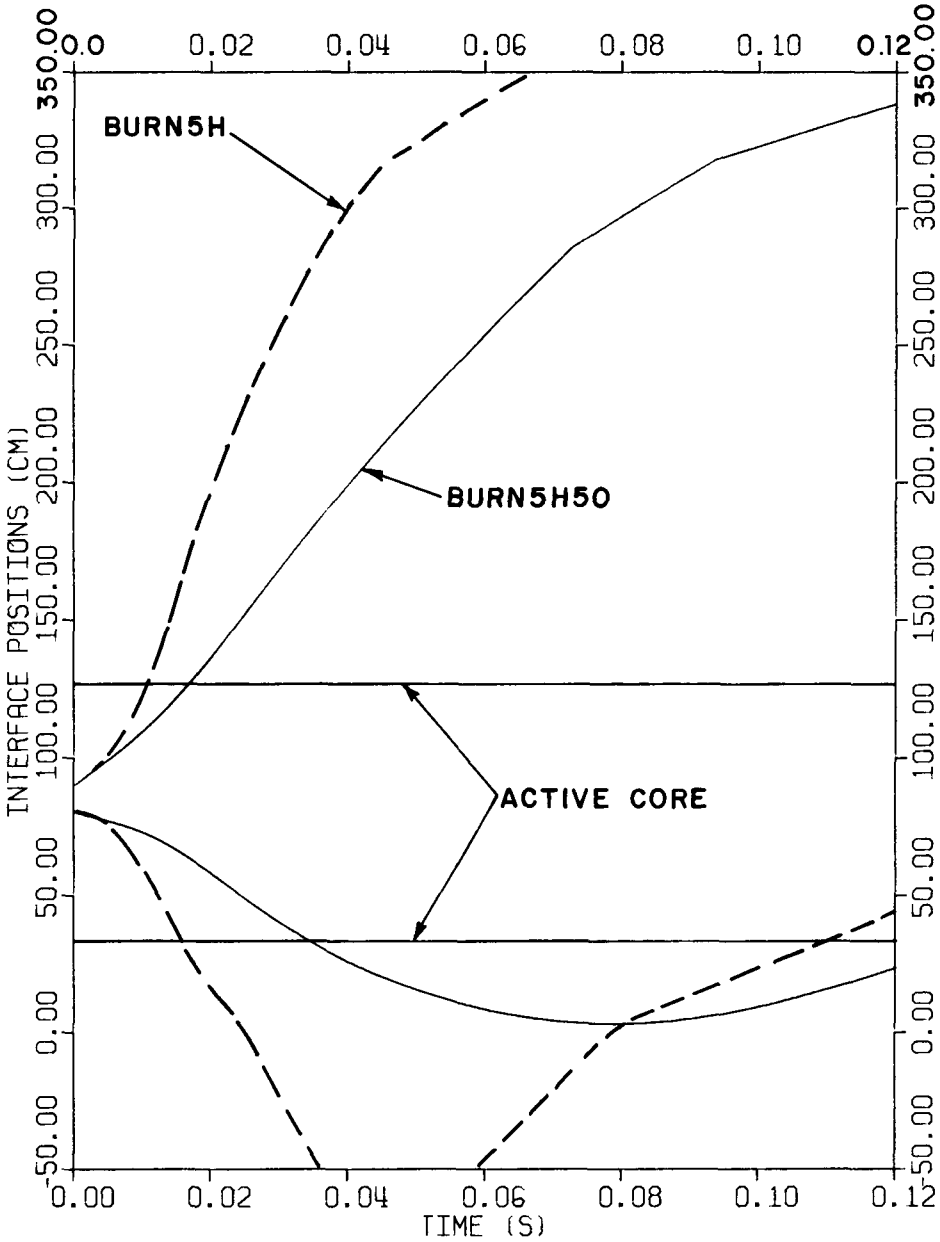

Figure 5.1 Subassembly Voiding Pattern Comparison for Energetic FCI Case; BURN5H50 Ejection Rate Reduced by Factor of Five from BURN5H Rate.

effects produced in parametric runs[7] by increasing the assumed fuel particle diameter by $\sqrt{10}$ or by halving the total mass of fuel ejected from the pin into the channel.

Having been unsuccessful at fundamentally changing the character of an energetic case, we decided to go to the other extreme and look at the effect of fuel ejection rates on a case which we knew would exhibit a much milder voiding behavior. The case selected (also described in Reference 7) was BURN8. This case was milder than BURN5H because of several code input differences. Only half as much fuel (4.8g) was ejected per pin, and only half as much sodium (0.8g) was involved. This simulated failure of only half the pins. Fuel particle diameters were larger by $\sqrt{10}$ (increased to 632 μm). Also the initial cladding temperature was higher by 100 K (1200 K). For comparison with BURN8, a case labeled BURN850C was run. Not only was the fuel ejection rate reduced by a factor of five from BURN8 (to a value of 0.105 g/ms/pin averaged over the entire subassembly), but a much larger mass of sodium (3.2 vs. 0.8g) was assumed to be involved, and the initial cladding temperature was also reduced to 1000 K. At the time the case was run, we were virtually certain that flow reversal would never be observed.

Figure 5.2 presents voiding histories for BURN8 and BURN850C. Certainly BURN850C is mild compared to BURN8, yet flow reversal eventually is achieved in BURN850C, and large void fractions are produced in the region around the initial failure site. At about 90 ms after FCI initiation (see Figure 5.2) the lower coolant slug had been pushed back down to its original location, and the average void fraction in the FCI zone was 0.8.

This behavior for such a potentially mild FCI is surprising at first glance; however, two considerations should be emphasized here. First, as indicated elsewhere in this report, the UVAFCI code used to analyze these situations loses validity when flow reversal is delayed. (That actually should not be a problem in the case BURN850C

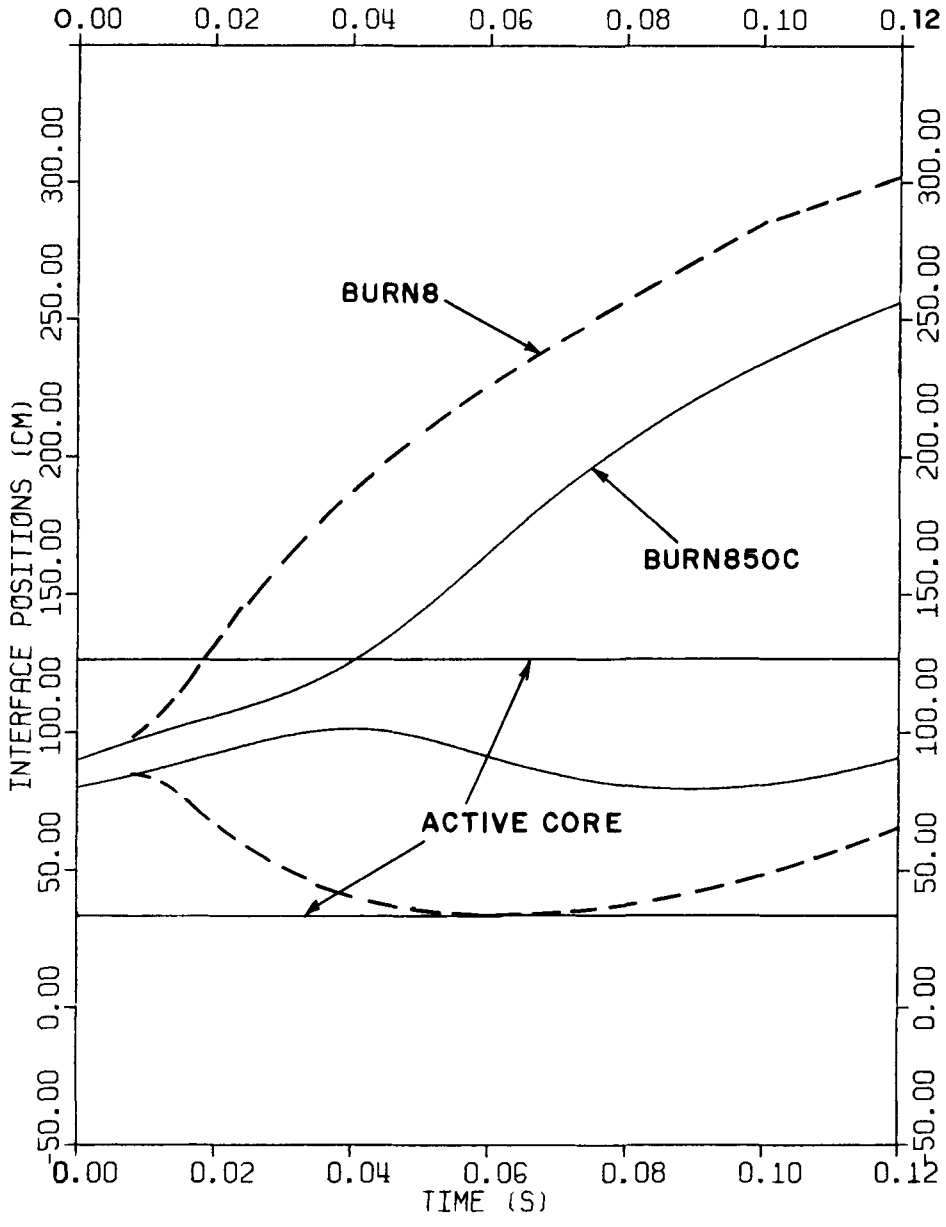

Figure 5.2 Subassembly Voiding Pattern Comparison for Mild FCI Case; BURN850C Ejection Rate Reduced by Factor of Five from BURN8 Rate.

presented here, because the larger mass of sodium utilized in the calculations was chosen on the basis of the delayed reversal.) A second consideration is the magnitude of the relative potential for voiding vs. continued upward motion and "sweepout" of the FCI zone. This latter consideration is very instructive, as seen below.

We have indicated previously[7] that, for long-term, extensive voiding, interaction zone temperatures and heat sink temperatures tend to converge. The zone pressure then is tied directly to this converged temperature through two phase equilibrium, and this pressure is crucial to establishing and maintaining voiding. These zone temperature and pressure arguments can explain why cladding/structure temperature at failure and total masses of both heat sink and fuel are so crucial to the FCI strength. A simple, illustrative calculation is given below.

A fuel mass of 10g is assumed to be ejected from each of half the pins in a CRBR subassembly and to reach equilibrium with an associated mass of steel and sodium. Based on the distance traveled in 100 ms by sodium moving at CRBR normal flow velocities of 6.7 m/s, consider the steel mass in a 67 cm length of subassembly ($\sim$ 7.5 Kg). Initial steel temperature is 1050 K. A sodium mass of 0.565 Kg (full flow for 25 ms) with an initial temperature of 1000 K is involved. After thermal equilibration of the fuel, steel, and sodium, the mixture temperature would be almost 1400 K, corresponding to a sodium vapor pressure of about six atmospheres - essentially the entire available driving pressure at the subassembly inlet. Thus, even with a calculation which takes full advantage of the heat sink available in about 75% of the active core height, substantial sodium pressures can be generated.

The above calculation shows then that we should have expected the results observed in BURN850C. Indeed, to guarantee that we eliminate flow reversal and voiding, fuel ejection rates must be so low that sodium entering the subassembly can effectively remove the energy of

the ejected fuel without reaching boiling. (This goes to the other extreme now of ignoring the massive structure heat sink). Average fuel ejection rates low enough to meet these requirements for initial fuel temperatures of 3100 K (just above liquids) and initial sodium temperatures of 700 K (just slightly higher than normal CRBR inlet flow) would be of the order of 0.01g fuel/ms/pin. Actual maximum fuel ejection rates which would avoid flow reversal would lie between the 0.01 value and the BURN850C value of 0.1 g/ms/pin. Other factors that characterize the FCI would, of course, come into play (e.g. assumed particle size), but it seems likely that fuel ejection rates which are conducive to benign fuel sweepout without excessive flow perturbations would be more than an order of magnitude smaller than the rates currently predicted by state of the art codes.

5.4 Modeling of Plenum Pressurization

In Section 4 of this report we presented a review of the ANL Upper Plenum Injection tests. After completing that review during this last fiscal year, we expended considerable effort looking at ways to model those tests and the potential plenum pressurization which is important to more prototypic reactor situations.

In general, the results of our modeling attempts were unsatisfactory. We found that any level of modeling which began to take into consideration most of the physical processes involved was becoming more sophisticated than either we wished or could hope to handle on the time frame available. Moreover, we found once again (as in our TOP-related FCI work) that the key rate processes in the time dependent analysis were ones of two phase, multi-component heat transfer between fuel and sodium. These rate processes are so little understood that we feel a parametric model would naturally grow out of any current attempt to model the plenum pressurization phenomena. Little would be gained from our working on such a model, especially when models such as SIMMER-I are available. Thus, although we will be discussing the results of some simple scoping calculations in the remainder of

this section, we would recommend that the emphasis for plenum pressurization analysis be placed on determination of the various exchange coefficients needed for a SIMMER mockup of the pressurization process.

In order to perform some scoping calculations of the possible pressures which might be produced in the ejection of a two-phase fuel mixture into a region containing sodium, a simple code called EQUILIB was written. The code input defines the total available volume, initial temperatures of fuel and sodium, and masses of fuel and sodium. Actual input parameters are arranged so that plenum geometry problems require only initial temperatures, initial void fraction, pin and wire wrap dimensions, flow area, and either mass of sodium or thickness of sodium film on pin and wrap.

The two-phase fuel is assumed to intimately mix with and attain instantaneous thermal equilibrium with the sodium present in the mixing volume. This gives an upper limit on possible pressures generated for two reasons: the resulting mixture is constrained to the mixing volume, and no heat transfer to structure is considered. The next logical extensions to the model would be to include simple time constants for heat transfer from fuel to sodium, sodium to structure, and fuel to structure, and to provide for expansion of the mixing zone against applicable constraints. However, as stated above, such extensions immediately increase the modeling sophistication and complexity to the point where the development of such a new model becomes unrealistic; rather the use of an existing model, e.g., SIMMER-I, seems more logical. At any rate, the results of our simple EQUILIB calculations will be presented here strictly as upper limits on potential pressurization.

The picture we worked from in setting up these calculations was one of a plenum region initially filled with sodium into which a two-phase (liquid and vapor) fuel mixture is injected. The fuel driving forces begin to void the sodium from the plenum region, leaving behind a sodium film (thickness $\sim$ .013 cm) on the structure surface.

The sodium was characterized by its initial temperature; the fuel was characterized by its initial temperature and void fraction (α). A series of calculations were run in which these three parameters were varied. The results of some of those calculations are shown in Table 5.1.

Case A was selected as a base case initially because it involved parameters which might characterize a very energetic situation, i.e., 4000 K fuel with $\alpha = 0.5$. The resulting pressure was enormous. It is worth noting that in Case A and all other cases except C and F the equilibrium temperature is above the critical temperature of sodium. Indeed, the melting temperature of the fuel (3040 K) is above the sodium critical temperature. Only for those cases (C and F) in which the void fraction, α, is taken as 0.99 do we end up with subcritical sodium.

As can be seen from the table, the results of varying initial sodium temperature, fuel temperature, and void fraction are consistent with what one would expect. It is especially interesting to look at Case F. The parameters in Case F, more than in other cases in the table, begin to approximate the plenum test conditions discussed in Section 4.5 of this report. The biggest difference is in the nature of the void region: fuel vapor in Case F vs. inert gas in the plenum injection test. Also heat sinks certainly would be acting in the tests, and confinement of the resulting fuel/sodium mixture would certainly be much less in the tests than modeled in EQUILIB.

Despite all these obvious differences which should cause EQUILIB to predict enormous pressures compared to the tests, the predicted pressure for Case F is only 1.05 MPa ($\sim$ 10.5 atm). This again emphasizes the importance of running more prototypic injection tests with fuel and sodium.

TABLE 5.1 Parametric Study with EQUILIB

CASE	Sodium		Fuel		Equilibrium		
	Initial Temp (K)	Mass (g/m/pin)	Initial Temp (K)	Mass (g/m(pin)	Initial Void Frac.	Temp (K)	Press (MPa)
A	1000	2.39	4000	64.6	0.50	3636	134
B	↓	↓	↓	13.0	0.90	3040	61.2
C	↓	↓	↓	1.24	0.99	1564	1.47
D	↓	↓	3500	66.8	0.50	3241	94.2
E	↓	↓	↓	13.3	0.90	3040	61.2
F	↓	↓	↓	1.34	0.99	1498	1.05
G	800	2.54	4000	13.0	0.90	2840	47.9
H	1200	2.24	4000	13.0	0.90	3040	59.7

SECTION 5 REFERENCES

1. C. A. Erdman and M. B. Johnson, "Some Aspects of Fuel Motion in the Unprotected Transient Overpower Accident in LMFBR's," NUREG-0282 (June 1977).

2. C. A. Erdman and M. B. Johnson, "Some Aspects of Subassembly Voiding in the Unprotected Transient Overpower Accident in LMFBR's," NUREG-0277 (June 1977).

3. R. N. Koopman et al., "TREAT Transient Overpower Experiment R9," Trans. Amer. Nucl. Soc., 24, 269 (1976).

4. Private Communication, R. N. Koopman.

5. H. U. Wider et al., "An Improved Analysis of Fuel Motion During an Overpower Excursion," Proc. ANS Fast Reactor Safety Conference, Beverly Hills, California, CONF-740401, pp. 1541-1555.

6. P. A. Pizzica and P. B. Abramson, "EPIC: A Computer Program for Fuel-Coolant Interactions," Proc. Int. Mtg. on Fast Reactor Safety and Related Fields, CONF-761001, Vol. III, pp. 979-987 (1976).

7. University of Virginia Annual Report for the Period July 1, 1975-June 30, 1976, NRC Contract No. AT(49-24)-0158.

8. L. L. Smith et al., "SIMMER-I, an LMFBR Disrupted Core Analysis Code," loc. cit. 6, pp. 1195-1202.